Variability and drivers of carbonate chemistry at shellfish aquaculture sites in the Salish Sea, British Columbia.

Eleanor Simpson[1], Debby Ianson[1,2], Karen E. Kohfeld[1,3], Ana C. Franco[4], Paul A. Covert[2], Marty Davelaar[2], Yves Perreault[5].

[1]Resource and Environmental Management, Simon Fraser University, Burnaby, British Columbia, Canada
[2]Insititute of Oceans Sciences, Fisheries and Oceans Canada, Sidney, British Columbia, Canada
[3]School of Environmental Science, Simon Fraser University, Burnaby, British Columbia, Canada
[4]Department of Earth, Ocean and Atmospheric Sciences, University of British Columbia, Vancouver, British Columbia, Canada
[5]Little Wing Oysters, Lund, British Columbia, Canada

Correspondence to: Eleanor Simpson (esimpson@sfu.ca)

Abstract.

Ocean acidification reduces seawater pH and calcium carbonate saturation states (Ω), which can have detrimental effects on calcifying organisms such as shellfish. Nearshore areas, where shellfish aquaculture typically operates, have limited data available to characterize variability in key ocean acidification parameters pH and Ω, as samples are costly to analyse and difficult to collect. This study collected samples from four nearshore locations at shellfish aquaculture sites on the Canadian Pacific coast from 2015–2018 and analysed them for dissolved inorganic carbon (DIC) and total alkalinity (TA), enabling the calculation of pH and Ω for all seasons. The study evaluated the diel and seasonal variability in carbonate chemistry conditions at each location and estimated the contribution of drivers to seasonal and diel changes in pH and Ω. Nearshore locations experience a greater range of variability and seasonal and daily changes in pH and Ω than open waters. Biological uptake of DIC by phytoplankton is the major driver of seasonal and diel changes in pH and Ω at our nearshore sites. The study found that freshwater is not a key driver of diel variability, despite large changes over the day in some locations. Shellfish mortality events coincide with highly favourable pH and Ω conditions during summer and are most likely linked to high surface temperatures and disease rather than ocean acidification. To reduce shellfish mortality, shellfish could be hung lower in the water column (5–20 m) to avoid high temperatures and disease, while still experiencing favourable pH and Ω conditions for shellfish.

1 Introduction

30 The ocean has absorbed approximately 30% of anthropogenic carbon dioxide (CO_2) from the atmosphere (Sabine et al., 2004; Gruber et al., 2019) which is the main driver of reduced surface ocean pH, a process known as ocean acidification (OA) (Calderia and Wicket, 2003; Raven et al., 2005). Increased oceanic uptake of CO_2 increases dissolved inorganic carbon (DIC) concentration and reduces pH, which shifts the equilibrium state such that the saturation states (Ω) of calcium carbonate minerals ($CaCO_3$), such as aragonite (Ω_a) and calcite (Ω_c) are decreased. The reduction in Ω has implications for calcifying

35 organisms (e.g., Orr et al., 2005; Kroeker et al., 2010). When $\Omega < 1$, $CaCO_3$ is more likely to dissolve; and $\Omega = 1$ is often used as a threshold to indicate stressful conditions for calcifying organisms, although stress has been observed at $\Omega_a \sim 1.5$ (e.g., Waldbusser et al., 2015; Gimenez et al., 2018). Lower Ω increases the energy expenditure required by calcifying organisms to build and maintain $CaCO_3$ structures (Spalding et al., 2017). Juvenile shellfish are particularly vulnerable to lower Ω (e.g., Waldbusser et al., 2015), as they use aragonite, which is a more soluble form of $CaCO_3$ (Mucci, 1983). Once settled, adult

40 shellfish transition to the less soluble form calcite (e.g., Stenzel 1964). Some of these negative impacts of OA are already being observed and could have wide-reaching consequences for ecosystems, human communities, and economies (e.g., Cooley et al., 2012; Ekstrom et al., 2015; Doney et al., 2020).

Although coastal areas are typically well populated by human communities and the nearshore is habitat for many organisms

45 vulnerable to OA, little is known about OA in the nearshore. Many calcifying species live and are farmed in nearshore (defined here as within 500 m of the low tide mark) estuarine environments, where pH and Ω are highly variable (e.g., Waldbusser and Salisbury, 2014), which makes identifying long-term trends challenging (Duarte et al., 2013; Fassbender et al., 2018). In addition to the absorption of atmospheric CO_2, variability in OA metrics pH and Ω in nearshore areas can be driven by a multitude of coastal factors (Waldbusser and Salisbury, 2014; Cai et al., 2021), including large temperature gradients, winds

50 and upwelling (e.g., Evans et al., 2019; Moore-Maley et al., 2017), freshwater and salinity change (Salisbury et al., 2008; Hu and Cai, 2013; Simpson et al., 2022), primary production or remineralization (Feely et al., 2010; Cai et al., 2011; Wallace et al., 2014; Pacella et al., 2018; Lowe et al., 2019), and anthropogenic activities resulting in acid deposition (Doney et al., 2007). The complexity of the nearshore environment, regionally specific drivers, a lack of data, and lack of models that resolve nearshore processes and variability, make predicting current conditions and future nearshore OA impacts challenging (e.g.,

55 Alin et al., 2015; Beaupré-Laperrière et al., 2020; Cai et al., 2020).

The Salish Sea is a large, productive, semi-enclosed, temperate, coastal sea, located on the Pacific coast of North America (Fig. 1a). The Strait of Georgia (SOG) is the largest water body in the Salish Sea, which mainly exchanges with the Pacific Ocean through Haro and Juan de Fuca Straits to the south (Pawlowicz et al., 2007), with limited exchange at the north (e.g.

60 Olson et al., 2020). Significant riverine inputs drive estuarine circulation in the SOG, which is composed of a Northern and Southern basin. These basins are two distinct biogeochemical zones (Jarníková et al., 2021) characterized by different physical

controls (Thomson, 1981; LeBlond, 1983; Pawlowicz et al., 2020). In the Southern Basin (SSOG), circulation is driven primarily by the glacial Fraser River (LeBlond, 1983; Pawlowicz et al., 2007), which is characterised by a strong spring-summer freshet. The circulation in the Northern basin (NSOG) is primarily driven by pluvial rivers (e.g., Puntledge River),

65 with peak discharge in winter (Morrison et al., 2011). As a result, the SOG is strongly stratified with a relatively fresh (salinities ~25 to 30) surface layer (~0 to 50 m), a lower layer with estuarine return flow (50 to 200 m), and a stagnant deep layer (~200 to 400 m), which receives deep water renewal in summer (Masson, 2002; Pawlowicz et al., 2007). Wind driven upwelling and mixing to the surface facilitates strong spring-summer phytoplankton blooms in the SOG which modulate pH and Ω seasonally (Moore-Maley et al., 2016; Evans et al., 2019;).

70

The sheltered coastline and summer phytoplankton abundance make the Salish Sea region ideal for shellfish growth (Silver, 2014; Holden et al., 2019), although shellfish mortality is a growing concern (e.g., Morin et al., 2020). The majority of shellfish aquaculture operations in the Salish Sea are located in the NSOG, in the Baynes Sound and the Discovery Islands regions (Holden et al. 2019). The relatively modest shellfish industry in the Salish Sea primarily grows Pacific Oyster (*Crassostrea*

75 *gigas*) and Manila Clams (*Venerupis philippinarim*) by obtaining seed from hatcheries (Banas et al., 2007; Barton et al., 2012; Haigh et al. 2015; Holden et al., 2019); and out-planting larvae or juveniles during spring-summer, in trays or bags on beaches, or suspended from rafts.

Shellfish mortality has become a global issue and a recurring challenge during summer in the Salish Sea, which has been
80 attributed to temperature and disease (King et al., 2019; Cowan, 2020; Morin, 2020), yet the role of changing carbonate chemistry conditions remains unknown. The SOG is DIC rich relative to the adjacent Pacific Ocean and already experiences low pH conditions (Ianson et al., 2016). The SOG has already undergone large changes since the pre-industrial period, with DIC increasing by up to ~40 μmol kg^{-1} (Evans et al., 2019; Jarníková et al., 2022; Simpson et al., 2022), shifting surface conditions from mostly Ω_a supersaturation to mostly Ω_a undersaturation, especially in winter (Jarníková et al., 2022). The
85 region is highly sensitive to increasing DIC (Hare et al., 2020; Simpson et al., 2022; Jarníková et al., 2022), and declines in Ω and pH from OA could be contributing to unfavourable Ω shell-forming conditions and shellfish mortality.

Here we investigate seasonal and diel biogeochemical variability at shellfish aquaculture sites in nearshore locations of the Canadian portion of Salish Sea and determine the key drivers of variability in pH and Ω, over a period of four years (2015 –
90 2018). We quantify the contributions of changes in salinity, temperature, biologically and salinity driven DIC, and total alkalinity (TA) changes to the seasonal and diel variability of pH, Ω_a and Ω_c. We investigate which drivers contribute the most to pH and Ω variability at each nearshore location and put the nearshore variability and drivers into context of the open waters of the SOG. As our study system is strongly stratified, we investigate two depth layers, the fresher surface layer (0 to 5 m) and a mid-layer (5 to 20 m), from which water could be mixed up into the surface layer. The surface layer is our focus, as most
95 shellfish are grown within this depth range and this portion of the water column experiences greatest variability.

2. Methods

2.1 Study Area

2.1.1 Okeover Inlet

Okeover Inlet (Fig. 1d) is located in the Discovery Islands region in the North Salish Sea. Okeover is a deep (~150 m), isolated
100 fjord with a narrow, shallow (~20 m) sill which restricts mixing with the outer waters of the NSOG. As a result, deep waters
in the inlet appear to have long residence times and are DIC rich (e.g., Simpson et al. 2022). Okeover Inlet is strongly stratified
in spring and summer, during which conditions are generally calm and glacial freshwater input from Theodosia River and
limited mixing contribute to low surface salinities. Strong stratification and high nutrient concentrations enable high primary
production, which supports significant aquaculture operations in the region. Winters can be cool and windy with occasional
105 storms that mix deep water to the surface. Despite higher winds, surface stratification persists through winter, as many small
pluvial creeks and streams feed into the inlet. Our study locations in Okeover Inlet are relatively small-scale, tray hang
operations (Fig. 1d, dark blue points) growing Pacific Oyster (*C. gigas*), as well as two beach locations (Fig. 1d, light blue
points). One of the beach locations in Okeover is a shell midden. Shell middens have been suggested as a possible adaption
technique for adapting to OA, as it is thought that dissolution of the shell hash will add TA back into the water and elevate pH
110 (e.g., Kelly et al., 2011).

2.1.2 Baynes Sound

Baynes Sound (Fig. 1 b, c) is a ~ 40 m deep channel between Vancouver Island and Denman Island in the NSOG. The majority
of the Canadian Pacific shellfish aquaculture operations are located in Baynes Sound (Holden et al., 2019), which is supported
by high spring-summer primary production. Production is high in this area as Baynes Sound is continually supplied with
115 nutrients from the north (Olson et al., 2020) and from deep water renewal from the south (Guyondet et al., 2022). The main
freshwater influence in Baynes Sound is the pluvial (i.e., winter peak) Puntledge River, which drives typical estuarine
circulation. Our sample site within Baynes Sound is located in Deep Bay, which is relatively shallow (~ 20 m) and rapidly
flushed, with residence times on the order of weeks (e.g., Guyondet et al., 2022). The sampling location is a large-scale tray
hang shellfish aquaculture operation growing primarily Pacific Oyster (*C. gigas*).

120 #### 2.1.3 Sansum Narrows

The Sansum Narrows region (Fig. 1e) is a narrow channel adjacent to the SSOG, located between Vancouver Island and Salt
Spring Island. It is connected to the SSOG through Satellite Channel, which feeds in well-mixed water from the turbulent Haro
Strait (e.g., Ianson et al., 2016). Exchange to the north end of Sansum Narrows is likely limited by shallow (~ 20 m) bathymetry
between the Gulf Islands. Rapid tidal streams and strong turbulent mixing through the narrow channel maintain a well-mixed
125 and relatively salty water column. As such, the strong stratification observed elsewhere in the Salish Sea is not observed in
Sansum Narrows, even in spring-summer during the Fraser River freshet (Waldichuk, 1957). The Fraser River plume likely

influences this region in spring-summer, but the main freshwater source is the pluvial (fall-winter peak) Cowichan River. Our sampling location in Sansum Narrows is a small-scale tray hang shellfish aquaculture tenure growing mostly Pacific Oyster (*C. gigas*).

130 **2.1.4 Evening Cove Beach**

We refer to a beach located north of Sansum Narrows, in Stuart Channel (Fig. 1e) as Evening Cove beach in this paper. Stuart Channel is less turbulent than Sansum Narrows, with slower tidal currents mostly less than 0.5 m s^{-1} at all depths (Waldichuk, 1964). Stuart Channel is strongly stratified and has strong freshwater influence from the Cowichan River in winter and some influence from the Fraser River in spring-summer. This beach location is a shellfish tenure, where both Pacific Oyster (*C.*

135 *gigas*) and Manila Clams (*V. philippinarim*) are grown in trays.
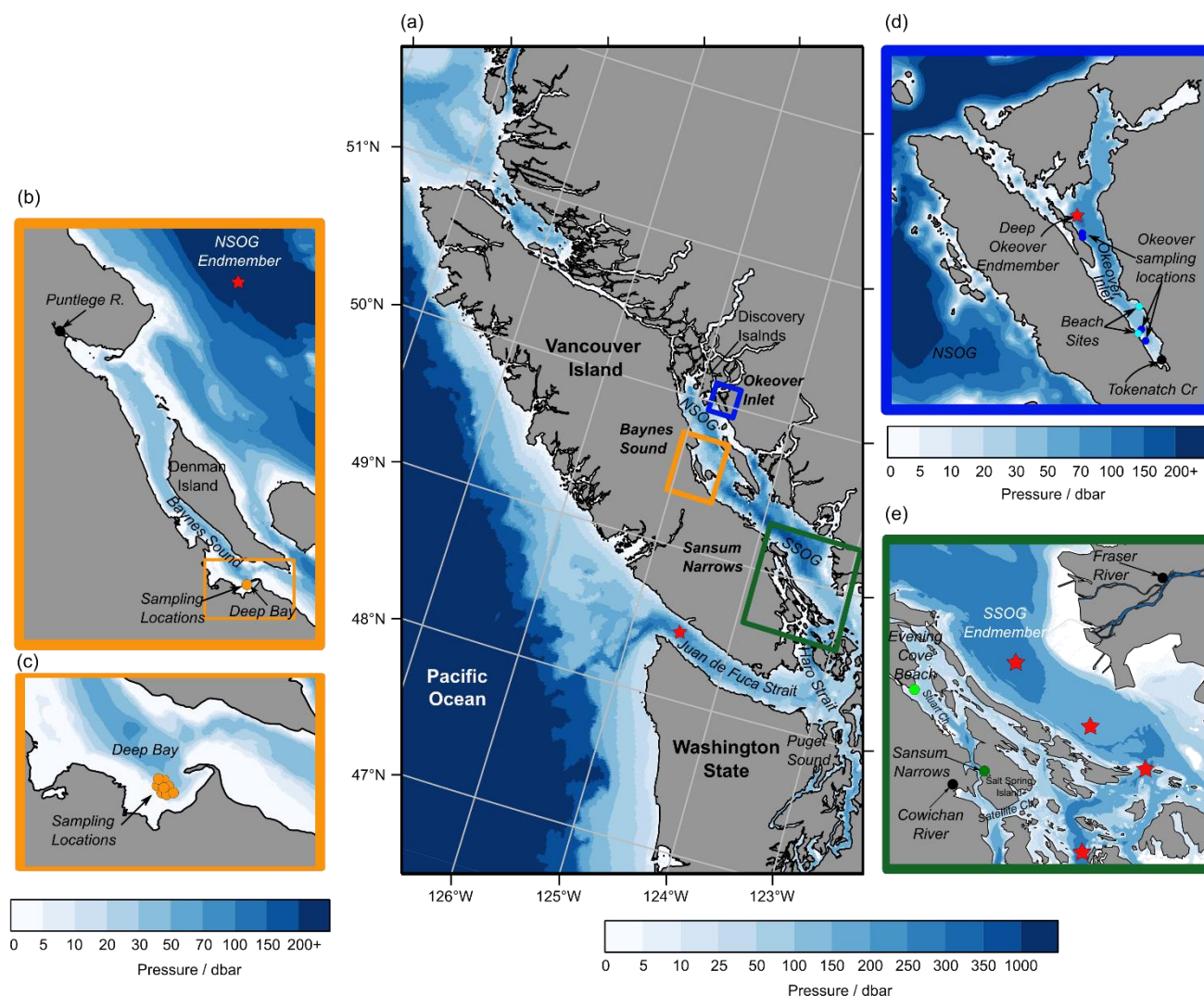
Figure 1. a) Sampling locations in the Salish Sea: Baynes Sound (orange), Okeover Inlet (blue) and Sansum Narrows (green). Multiple
140 nearshore sites at shellfish leases were sampled at each location as well as freshwater endmembers (black) and sub-surface salty endmembers
(red stars) (b-e) (Tables A1 and A2). b) Baynes Sound, showing nearshore sampling locations in Deep Bay (orange), the Puntledge River
freshwater endmember (black) and NSOG salty endmember (red star). c) Deep Bay nearshore sampling locations at a tray hang lease. d)
Okeover Inlet, showing nearshore sampling locations taken at tray hang shellfish leases (dark blue) and beach grow sites (light blue), the
freshwater endmember - Tokenatch creek - (black) and the deep-water salty endmember (red star). e) Sansum Narrows showing nearshore
145 shellfish lease sampling location (dark green) and beach grow site "Evening Cove beach" (light green) at Coffin Point in Stuart channel, the
Cowichan River freshwater endmember for this region and the Fraser River freshwater endmember for the SOG region (black) and the four
stations that were used to determine the SSOG salty endmember (red stars). *Credit: NE Pacific bathymetry from NOAA (2009), shorelines
from NOAA (2017) and Baynes Sound bathymetry from Natural Resources Canada (2021).*

150

2.2 Data collection and sample analysis

We collected discrete water samples from the Salish Sea for analysis of dissolved inorganic carbon (DIC), total alkalinity (TA), salinity (S), dissolved oxygen (DO) and nutrients (silicic acid, nitrate, and phosphate) over 20 campaigns spanning all seasons from 2015 – 2018. We sampled nearshore locations in Okeover Inlet, Baynes Sound, Sansum Narrows, and Evening Cove
155   beach (Fig. 1). Sample locations were mostly active shellfish grow sites, including beach grow sites and tray hangings. Due to the strong stratification of our study system, Niskin bottles were used to collect samples from the surface layer (0 to 5 m), within the mid-depth layer (5 to 20 m) and near bottom (away from beaches depth varied by location ~30–100 m). Niskin bottles were deployed from small skiffs or at beaches they were triggered by hand after wading in from shore. Conductivity, temperature and depth (CTD) profiles were taken simultaneously in the water column (Simpson et al., 2022). We sampled
160   throughout the day at most locations, starting in the morning (~7 to 8 am) and concluding mid-afternoon (~4 to 5 pm). We took samples at least once during ebb, slack, and neap tides. No night-time samples were collected, assuming that the morning samples contain the maximum diel respiration signal. Sample collection and analysis followed standard procedures (Barwell-Clarke and Whitney, 1996; Carpenter, 1965; Dickson et al., 2007 and WOCE, 1991; see Simpson et al., 2022, A2 for sample analysis detail).

165

Understanding the variability within these estuarine systems requires that we first characterize the waters that are entering and mixing from both freshwater and salty sources at each location. To do this, we characterised the freshwater and salty-water endmembers at each location. We collected discrete samples of DIC, TA, S, DO and nutrients as well as CTD readings from local freshwater sources and from locations that are representative of the salty water that mixes into each study location (Table
170   A1). Endmembers were selected based on the fit of observational data collected in the region to endmember salinity gradients (i.e., how well observational data fit the mixing line between fresh and salty endmembers) for Baynes Sound and Okeover Inlet (Simpson et al., 2022), and in Sansum Narrows and Evening Cove beach (A1).

To calculate pH, Ω_a and Ω_c we used the observed DIC, TA, silicic acid, phosphate, bottle salinities, and CTD temperature and
175   pressure to solve the carbonate system (full details in Simpson et al., 2022) using CO2sys (van Heuven et al., 2011; Lewis and Wallace, 1998) with Millero (2010) carbonate constants, Dickson (1990) KSO_4 constants, and Uppström (1974) borate constants. Data were also divided into two seasons: a productive season capturing the regional phytoplankton blooms (April-September) subsequently referred to as "summer' and less productive season (October-March) referred to as "winter".

2.3 Salinity Normalisation

180

Normalised DIC and TA were estimated following Friis et al. (2003) using a regionally derived DIC-S and TA-S relationship for each study sub-region (Fig. 1) established from site specific endmembers (Table A2) and the mean annual salinity ($\overline{S}_{annual}$), not weighted by season, at the location and depth range of interest (Table A3). Where available, the freshwater intercept for each DIC-S and TA-S relationship was determined directly from observations; where no freshwater data were available, we

185 extrapolated to S=0 using the salinity relationship established for that location from the data available (Simpson et al., 2022). Normalising DIC and TA to $\overline{S}_{annual}$ (DIC$_{\overline{s}}$ and TA$_{\overline{s}}$) removes changes in these parameters resulting from dilution. In this region, the remaining variability can be attributed to biological processes (Simpson et al., 2022). We calculate the difference between the winter and summer mean DIC$_{\overline{s}}$ and TA$_{\overline{s}}$, to give the seasonal difference in DIC (ΔDIC$_{\overline{s}}$) and TA (ΔTA$_{\overline{s}}$) resulting from biological processes.

2.4 Drivers of seasonal change in pH and CaCO₃ saturation state

190

We estimate the individual contributions of biological processes, temperature, and freshwater to seasonal changes in pH, Ω_a and Ω_c (ΔpH, $\Delta\Omega_a$ and $\Delta\Omega_c$) at each location and depth, using a first order Taylor expansion (e.g., Sarmiento and Gruber, 2006; Lovenduski et al., 2007; Turi et al., 2016; Franco et al., 2021) (eqs. 1– 3):

195
$$\Delta pH \approx \frac{\partial pH}{\partial DIC}\Delta DIC_{\overline{s}} + \frac{\partial pH}{\partial TA}\Delta TA_{\overline{s}} + \frac{\partial pH}{\partial T}\Delta T + \frac{\partial pH}{\partial fw}\Delta fw \tag{1}$$

$$\Delta \Omega a \approx \frac{\partial \Omega a}{\partial DIC}\Delta DIC_{\overline{s}} + \frac{\partial \Omega a}{\partial TA}\Delta TA_{\overline{s}} + \frac{\partial \Omega a}{\partial T}\Delta T + \frac{\partial \Omega a}{\partial fw}\Delta fw \tag{2}$$

$$\Delta \Omega c \approx \frac{\partial \Omega c}{\partial DIC}\Delta DIC_{\overline{s}} + \frac{\partial \Omega c}{\partial TA}\Delta TA_{\overline{s}} + \frac{\partial \Omega c}{\partial T}\Delta T + \frac{\partial \Omega c}{\partial fw}\Delta fw \tag{3}$$

The first and second terms on the righthand side of eqs. 1–3 represent the contribution of biologically driven changes in DIC

200 and TA, to ΔpH, $\Delta\Omega_a$ and $\Delta\Omega_c$, respectively. The third term is the contribution of seasonal temperature difference (ΔT), the difference between mean winter and mean summer T, to ΔpH, $\Delta\Omega_a$ or $\Delta\Omega_c$. The final term is the freshwater component (fw), defined in eqs. 4–6.

Partial derivatives measure the sensitivity of pH and Ω to a small change in one environmental variable when all other

205 carbonate system parameters (i.e., TA, T, and S) are held constant. For example, the partial derivatives $\frac{\partial pH}{\partial DIC}$, $\frac{\partial \Omega a}{\partial DIC}$, $\frac{\partial \Omega c}{\partial DIC}$ in eqs. 1–3 measure how much pH, Ω_a and Ω_c respond to a small change in DIC. We calculate partial derivatives of Ω_a and Ω_c (Table A4) using the Derivnum function in CO2sys (Orr et al., 2018). At the time of writing, there is no function in Derivnum to calculate partial derivatives of pH. We calculated the partial derivatives of pH using the same finite step sizes used in Derivnum to calculate partial derivatives of Ω_a and Ω_c and re-solved the system using CO2sys (Appendix A2).

210

To calculate the total seasonal ΔpH, $\Delta\Omega_a$ and $\Delta\Omega_c$, we multiply partial derivatives with the observed seasonal changes in each individual driver, i.e., biologically driven DIC ($\Delta DIC_{\bar{s}}$), biologically driven TA ($\Delta TA_{\bar{s}}$), seasonal temperature change (ΔT) and seasonal freshwater contribution (Δfw). The seasonal differences in DIC and TA are normalised to the annual mean salinity (Table 1).

215

The contribution of seasonal changes in freshwater to ΔpH, ΔΩa or ΔΩc is defined as:

$$\frac{\partial pH}{\partial fw}\Delta fw \approx \frac{\partial pH}{\partial S}\Delta S + \frac{\partial pH}{\partial TA}\Delta TA_{fw} + \frac{\partial pH}{\partial DIC}\Delta DIC_{fw} \tag{4}$$

$$\frac{\partial \Omega a}{\partial fw}\Delta fw \approx \frac{\partial \Omega a}{\partial S}\Delta S + \frac{\partial \Omega a}{\partial TA}\Delta TA_{fw} + \frac{\partial \Omega a}{\partial DIC}\Delta DIC_{fw} \tag{5}$$

220 $$\frac{\partial \Omega c}{\partial fw}\Delta fw \approx \frac{\partial \Omega c}{\partial S}\Delta S + \frac{\partial \Omega c}{\partial TA}\Delta TA_{fw} + \frac{\partial \Omega c}{\partial DIC}\Delta DIC_{fw} \tag{6}$$

The first term on the righthand side of eqs. 4–6 is the contribution of seasonal S differences (ΔS) to seasonal ΔpH, $\Delta\Omega_a$ and ΔΩ, arising from the salinity dependence of carbonate system constants (e.g., Millero, 2006); where ΔS is the difference between mean winter S ($\bar{S}_{winter}$) and mean summer S ($\bar{S}_{summer}$). The final two terms, ΔDIC_{fw} and ΔTA_{fw}, in eqs 4–6, represent

225 the change in DIC and TA driven by seasonal salinity change (ΔS), or in other words, dilution. To calculate ΔDIC_{fw} and ΔTA_{fw} we used regionally specific DIC-S and TA-S relationships to estimate the change in DIC and TA along the salinity gradient resulting from salinity change with freshwater input (ΔS). We estimate uncertainty in the Taylor expansion results from both derivative and seasonal change uncertainties (A3). The unusual coccolithophore bloom that occurred in Okeover in 2016 (NASA, 2016) has been excluded from the seasonal analysis, as it was an anomalous event spanning a shorter temporal

230 scale, lasting days to weeks. It is, however, included in the diel analysis.

2.5 Diel drivers of pH and CaCO₃ saturation state

We also investigate the drivers of diel variability at locations where sufficient observations were made during both the morning and afternoon to capture changes in carbonate chemistry throughout the day. Specifically, we required sampling over a minimum of 6 hours, capturing morning, noon, and afternoon at a given day and location. We selected a day from both the

235 summer and winter season at each site for analysis (Table 2). When multiple days fulfilled this requirement at a particular location, we analysed the day that had the greatest range in conditions or drivers of pH and Ω. The winter day chosen for Baynes Sound was selected due to a large range in salinity observed throughout the day. While a large winter diel salinity range is not necessarily representative of everyday conditions in Baynes Sound, we chose the day with the greatest range to investigate the importance of freshwater as a potential diel driver of carbonate chemistry conditions. The summer day selected

240 for Okeover beach was the only day meeting our criteria for diel analysis and captures the unusual coccolithophore bloom that occurred in 2016 (NASA, 2016; Simpson et al., 2022).

We estimate the diel contribution of drivers of pH, Ω_a and Ω_c variability in the surface layer only (0–5 m), as we sampled the surface layer more frequently and captured samples from the same location throughout the day. We estimate the diel drivers using eqs. 1–6, using the same partial derivatives calculated for the seasonal Taylor analysis (Table A4), but here we use the difference in DIC, TA, T and S observed over a single day (Table 2) rather than season. We estimate the biologically driven diel ΔDIC and ΔTA in eqs. 1–3, using the change in $DIC_{\bar{s}}$ and $TA_{\bar{s}}$ over the day. The freshwater component (eqs. 4–6) was estimated using the DIC-S and TA-S relationships calculated for each location (as above), with the observed diel range in salinity (ΔS). $DIC_{\bar{s}}$ and $TA_{\bar{s}}$ were normalised to $\bar{S}_{annual}$, for the depth and location of interest as above, following Friis et al. (2003) (Sect. 2.2). We keep the salinity normalisation the same for the diel and seasonal analysis (i.e., rather than normalising to a seasonal salinity) to avoid shifting to a point in carbonate space with different sensitivity (e.g., Egleston, 2010; Hu and Cai, 2013; Simpson et al., 2022). Thus, results from the seasonal and diel Taylor analyses, and the winter and summer diel analyses, may be directly compared.

255

3. Results
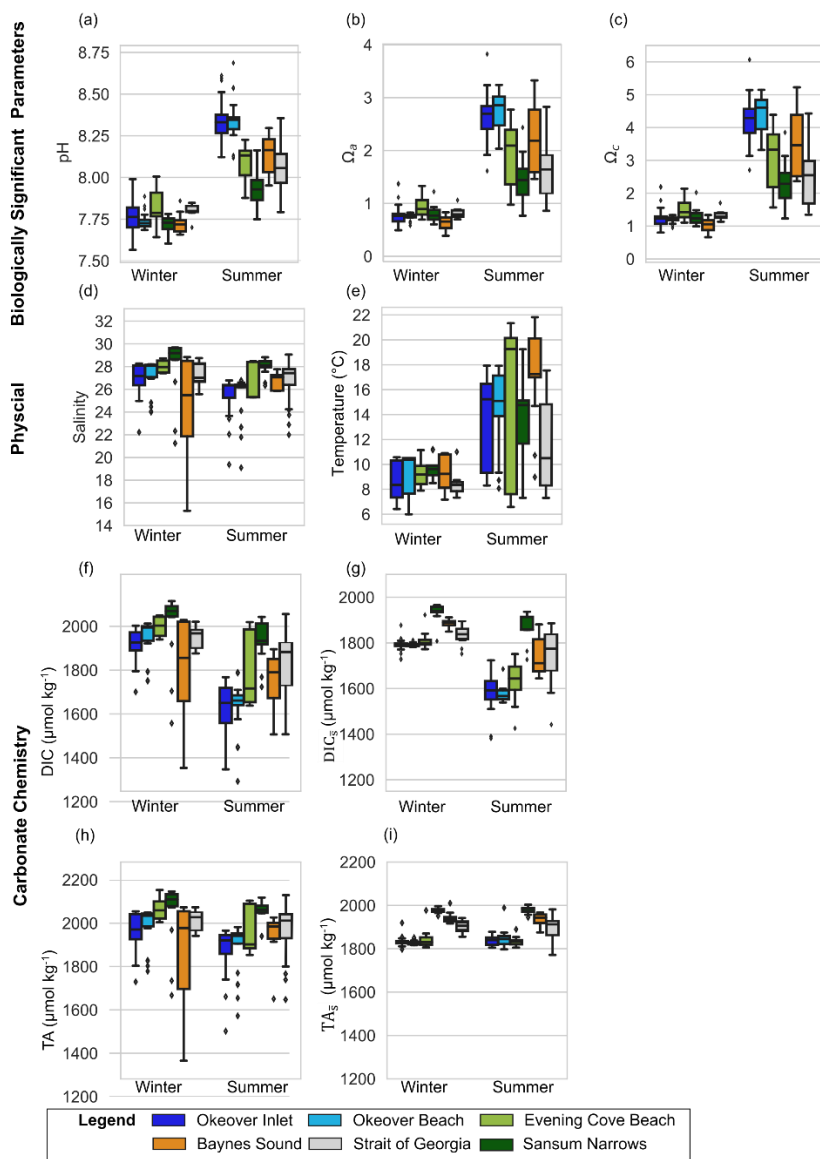
Figure 2 Observed variability at shellfish grow sites and adjacent waters in the surface layer (0-5 m) in winter and summer, respectively in a) pH, b) Ω_a, c) Ω_c, d) salinity, e) temperature, f) DIC, g) salinity normalized DIC (**DIC$_{\bar{s}}$**), h) TA, and i) salinity normalized TA (**TA$_{\bar{s}}$**), at nearshore locations shown in Fig. 1: Okeover (dark blue), Okeover beach (light blue), Evening Cove beach (light green), Sansum Narrows (dark green), Baynes Sound (orange) and ship collected data from the SOG (grey). Data have been split into a summer season capturing phytoplankton blooms (April-September) and winter season (October-March). The mean annual salinity (Table A3) at each location was used to normalize DIC and TA, to show the impact of dilution. There is inter-seasonal variability at all locations and generally greater variability and range of conditions during the summer season, with the exception of salinity during the winter season in Baynes Sound. Boxes represent the interquartile range in conditions, middle bars are the median value and outer bars the full range in values, and points are outliers. The number of samples used to generate plots is given in Table A8.
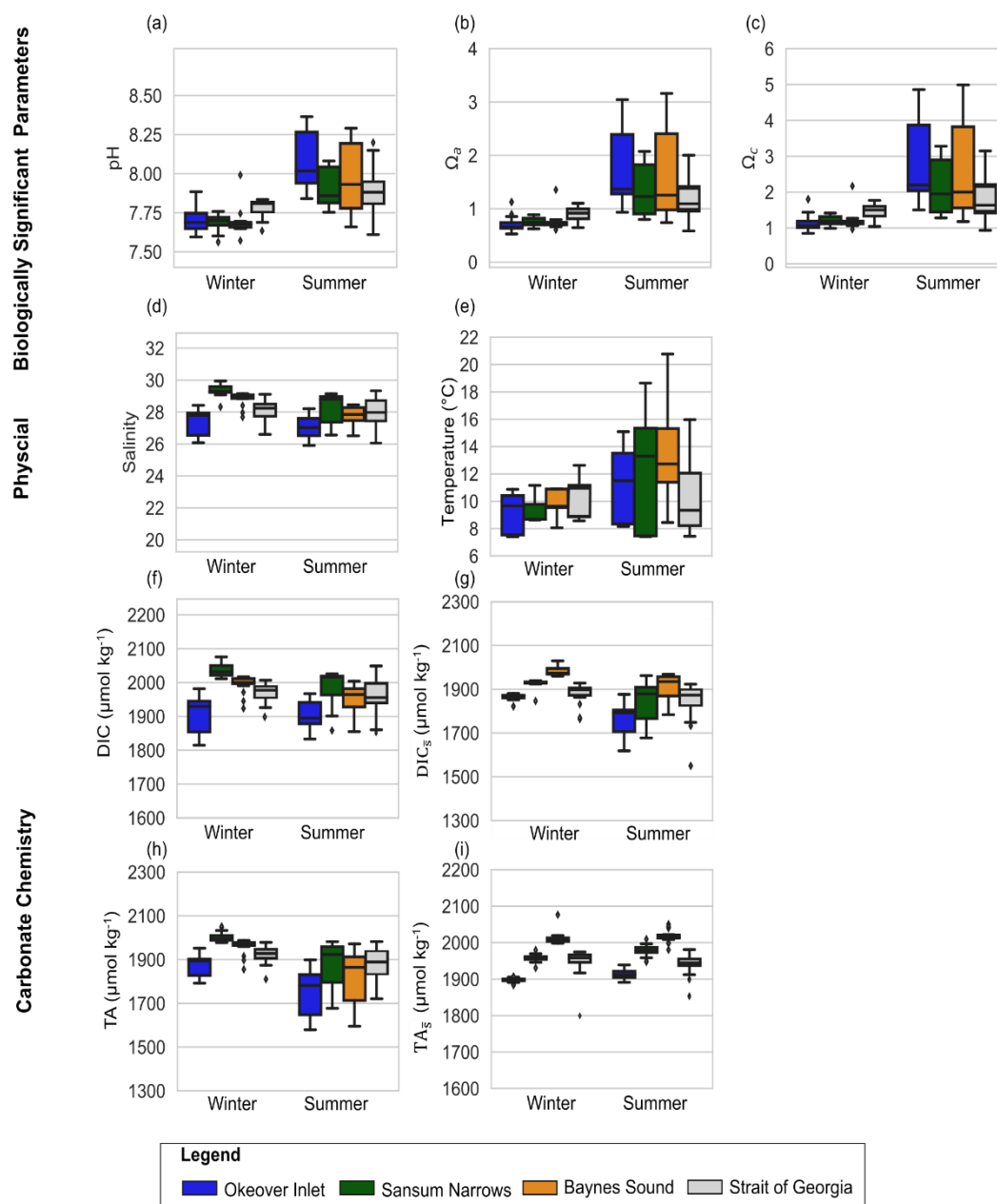
Figure 3 Observed variability in the 5-20 m layer at shellfish grow sites and in adjacent waters in a) pH, b) Ω_a, c) Ω_c, d) salinity, e)
temperature, f) DIC, g) salinity normalized DIC (**$DIC_{\bar{s}}$**), h) TA, and i) salinity normalized TA (**$TA_{\bar{s}}$**), at nearshore locations shown in Fig. 1:
Okeover (dark blue), Sansum Narrows (dark green), Baynes Sound (orange) and ship collected data from the SOG (grey). Data have been
split into a summer season capturing the phytoplankton bloom (April-September) and winter season (October-March). The mean annual
salinity (Table A3) at each location was used to normalize DIC and TA to show the impact of dilution. Similar to the surface layer, there is
inter-seasonal variability at all locations and greater variability and range of conditions during the summer season. There is lower variability
in conditions in the mid-layer than in the surface. Boxes represent the interquartile range in conditions, middle bars are the median value,
outer bars the full range in values, and points are outliers. The number of samples used to generate plots is given in Table A8.
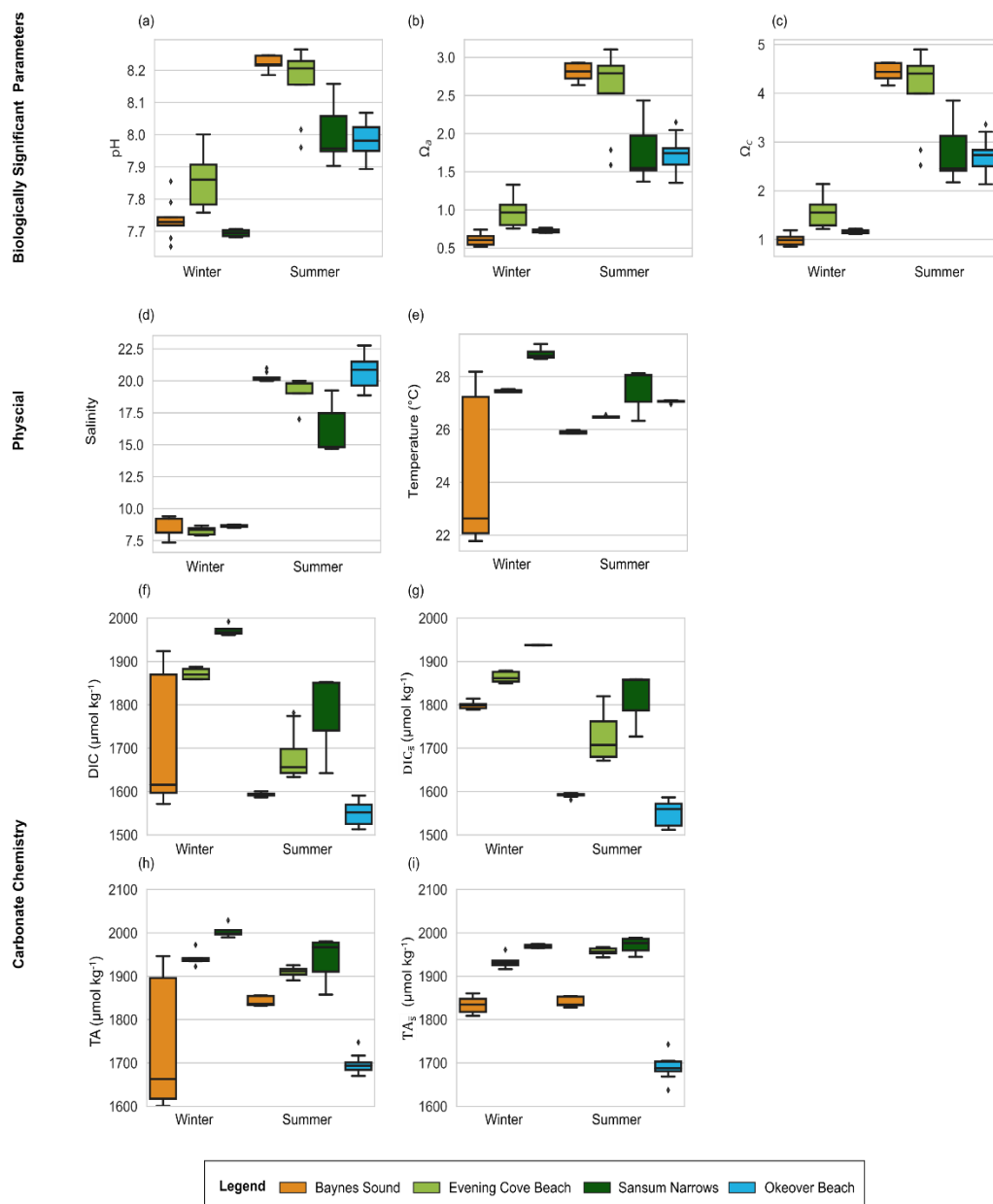
Figure 4 Variability during one sampling day (Table 2) at Baynes Sound (orange), Evening Cove beach (light green) and Sansum Narrows (dark green) for both summer and winter, and Okeover beach (light blue) in summer only, in a) pH, b) Ω_a, c) Ω_c, d) salinity, e) temperature, f) DIC, g) salinity normalized DIC (**DIC$_{\bar{s}}$**), h) TA, and i) salinity normalized TA (**TA$_{\bar{s}}$**),in winter (left) and summer (right). The mean annual salinity (Table A3) at each location was used to normalize DIC and TA (e,h) to show the impact of dilution. Boxes represent the interquartile range in conditions, middle bars are the median value, outer bars the full range in values, and points are outliers.

285

3.1 Seasonal Variability

At each nearshore location, variability in both chemical and physical properties around the median (Figs 2 and 3) is particularly strong at the surface and in summer. The open-water SOG region also has high variability in summer as it covers a large geographical extent including both the distinct NSOG and SSOG basins, which includes the Fraser River plume. However, the

290   open-water SOG has lower median pH and Ω than the nearshore in summer, and slightly higher pH and Ω in winter. When the nearshore sites are considered collectively as the nearshore environment of the Salish Sea region, they experience greater variability than the open waters of the SOG in both winter and summer. Okeover Inlet, in particular, has high pH and Ω that contribute substantially to the larger range in carbonate chemistry conditions in the nearshore.

3.1.1 Temperature

295   **Surface Temperature**

Surface temperatures are low and experience modest variability across all locations in winter (Fig. 2e) ranging from ~6 to 11 °C. All sites have a similar median temperature (~9 °C), although Okeover Inlet in our data is slightly cooler than other nearshore locations. Sansum Narrows, where tidal mixing is strong, has the lowest surface T variability of the nearshore

300   locations.

In summer, surface-water temperatures are higher (median ~15 to 19 °C) and more variable, reaching up to 22 °C in Baynes Sound and Evening Cove beach. The summer range in surface temperatures is particularly large at Evening Cove beach and Sansum Narrows, ~ 6 to 22 °C. In our observations, maximum temperatures in Baynes Sound are the highest, and although

305   some lower temperature observations are present, they typically do not extend into the cooler range observed elsewhere. Regardless, highest median summer temperatures are found at Evening Cove beach. We observe coolest minimum summer temperatures in Okeover Inlet, where temperatures do not exceed 18 °C, with the exception during coccolithophore bloom when summer temperatures were unusually high (up to 22 °C). Sansum Narrows median temperature is marginally cooler than Okeover, making it the coolest nearshore location in summer. Although summer surface temperatures exhibit a similar range

310   in the SOG and nearshore sites, median summer surface temperature in the SOG is 4 to 7 °C cooler than in the nearshore in our observations.

Mid-layer Temperature

Mid-layer temperatures are also cooler in winter than in summer and exhibit lower variability than the surface temperatures

315   (Fig. 3e). Winter median temperatures in the nearshore are typically slightly higher (~1°C) in the mid-layer than in the surface, and conversely in summer, mid-layer temperatures are ~4 °C lower than in the surface. Variability in mid-layer temperatures

in the nearshore is low in winter and higher in summer. Nearshore mid-layer variability is lower than in the surface in summer, ranging from 8 to 20 °C, but similar to the surface in winter. Mid-layer median temperatures in the SOG are lower than in the nearshore in summer, and slightly higher than the nearshore in winter.

3.1.2 Salinity

Surface salinity

Each nearshore location has a different salinity median and range, in both winter and summer. At all sites, winter surface salinities appear to be slightly higher than they are in summer, but the median and variability are similar in both seasons (Fig. 2d). In our observations, the lowest median surface winter salinities (~25) are found in Baynes Sound. Winter salinities are higher in Okeover (including beach sites) and at the Evening Cove beach site ~ 27 to 28. The highest median winter salinities are found in Sansum Narrows ~ 29, which is even higher than the median salinity in the SOG (~27). The most prominent surface salinity variability (ranging from 15 to 29) is seen in Baynes Sound during the winter, where we observed strong stratification with a lower salinity brackish lens on several occasions. Winter surface variability across the remaining nearshore locations is moderate (ranging by ~2). The nearshore sites exhibit a greater range in salinity than the SOG, but median salinities are similar, with the exception of the particularly low median salinity in Baynes Sound in our data.

Surface salinities are typically lower (~2) in summer than in winter (Fig. 2d), and Okeover is fresher than any other nearshore location in summer. Salinity ranges at nearshore sites are similar in both seasons, with the exception of Baynes Sound, which exhibits a large salinity range in winter, but not in summer. Nearshore salinity ranges are similar to the SOG region in summer, although some fresher measurements are found in Okeover. The SOG region encompasses a large geographical area, including locations of high and low salinities; for example, lower salinities in the SSOG in summer (<25) can be attributed to the Fraser River freshet.

Mid-layer salinity

Like the surface, mid-layer salinities in the nearshore are also slightly fresher in summer than in winter (Fig. 3d). In both seasons, median mid-layer salinity is about 1 to 2 units saltier than the surface at all sites except for Sansum Narrows, where salinities are similar in both the surface and mid-layer. Summer variability in salinity in the mid-layer is lower than at the surface in the nearshore and in the SOG region.

3.1.3 DIC and TA

Surface DIC and TA

Surface median DIC and TA are higher in winter at all sites (Fig. 2f and 2h) and nearshore medians and ranges are similar to those in the SOG. Sansum Narrows has the highest winter median DIC and TA of all locations, including the SOG. Winter DIC and TA ranges are relatively low compared to summer and are similar across sites, including the SOG (~ 100 to 200 µmol

kg⁻¹), except for in Baynes Sound where DIC and TA exhibit a large range of ~700 µmol kg⁻¹. Winter DIC and TA at our
350 locations are highly salinity dependent (Simpson et al., 2022), as median values and ranges of DIC and TA at each site follow
a similar pattern to salinity (Fig. 2d). The large winter range in DIC and TA observed in Baynes Sound is a result of the
exceptional salinity range at this location.

Summer median DIC and TA in the surface are typically much lower than in winter in the nearshore. This seasonal difference
355 is minimal in Sansum Narrows, and even smaller in the SOG (Fig. 2f, h). Nearshore summer median DIC and TA are generally
much lower than in the SOG and are particularly low in Okeover Inlet. Median DIC and TA in Sansum Narrows, however, are
the highest of the nearshore locations and are also higher than in the SOG. Typically, larger ranges in DIC are found at
nearshore sites in summer than winter, with the exception of Baynes Sound, where a larger, salinity-driven range in DIC and
TA occurs in winter. A large range in summer DIC and TA is also found in the SOG, which encompasses most of the conditions
360 found at the nearshore sites but does not capture the low DIC and TA observed in Okeover.

When DIC and TA are normalised to the annual mean salinity, the ranges in winter and summer DIC$_{\bar{s}}$ and TA$_{\bar{s}}$ shrink,
especially in winter (Fig. 2g and 2i). The range in summer TA$_{\bar{s}}$ also shrinks, while the range in summer DIC$_{\bar{s}}$ remains relatively
large. The small range in winter and summer TA$_{\bar{s}}$, and winter DIC$_{\bar{s}}$, indicates the predominant salinity dependence of winter
365 DIC variability and year-round TA variability. The salinity dependence of DIC variability is not as strong in summer when
other processes, such as primary production, contribute to variability (Simpson et al., 2022).

Mid-layer DIC and TA
Mid-layer DIC and TA are higher than in the surface, in both winter and summer (Fig. 3f and 3h). Median mid-layer winter
370 and summer TA are ~40 to 50 µmol kg⁻¹ higher than surface medians. Winter mid-layer DIC is also ~40 to 50 µmol kg⁻¹ higher
than the surface, but in summer mid-layer DIC is much higher than the surface (150 to 220 µmol kg⁻¹), especially in Baynes
Sound and Okeover Inlet. The higher DIC seen in the mid-layer at these locations is not as prominent in the tidally mixed
Sansum Narrows, where DIC in the mid-layer is ~80 µmol kg⁻¹ higher than the surface. Variability in mid-layer DIC and TA
in winter is similar to the variability seen in the surface, except for in Baynes Sound where the large variability in the surface
375 is not seen in the mid-layer. Summer variability in the mid-layer is greater than in winter, is similar across nearshore sites (a
range of ~ 300 µmol kg⁻¹), and is far less than the variability observed in the surface. When normalised to the annual mean
salinity, the range in mid-layer year-round TA$_{\bar{s}}$ and winter DIC$_{\bar{s}}$ is small. The range in summer DIC$_{\bar{s}}$, however, remains
moderate. The small range in TA$_{\bar{s}}$ and winter DIC$_{\bar{s}}$ indicates that the variability of TA throughout the year, and winter DIC,
are highly dependent on salinity. The salinity dependence of DIC in summer is not as strong, and primary production is
380 contributing to variability through the surface and into the mid-layer in the productive months (Simpson et al., 2022).

3.1.4 pH

Surface pH

Winter surface pH values at nearshore sites are all much lower than they are in summer, ranging from ~7.6 to 8.1 across all
385   locations (Fig. 2a). Median surface pH varies little across nearshore sites in winter, which is ~7.75 at all locations; and
nearshore pH is lower than in the SOG region where the median pH is 7.85. Winter surface pH range is largest in Okeover
Inlet and at Evening Cove beach (~0.4), and these ranges are similar in both winter and in summer. At other nearshore locations,
winter surface pH variability is smaller (~0.15) and less variable than summer.

390   Nearshore summer pH ranges are higher than in winter (~0.4 across nearshore sites), but these summer ranges are smaller than
pH range in the   SOG region. However, when considering all nearshore sites collectively as the nearshore environment of the
SOG, the total range in pH is 7.75 to 8.6, making summer surface pH variability at the nearshore significantly larger than open
water variability.

395   Nearshore summer median pH is high, especially in Okeover Inlet, where median surface pH is ~8.3 (Fig. 2a). Okeover Inlet
also experiences the highest summer pH of the nearshore locations, reaching a maximum pH of ~8.6 within the inlet and ~8.7
at the beach. Sansum Narrows has the lowest summer pH of ~ 7.85, with low pH values comparable to winter conditions at
other nearshore locations. Typically, lower pH at nearshore locations corresponds with higher DIC (Fig. 2f). Interestingly,
however, the large DIC range seen in Baynes Sound in winter does not result in a similarly large range in pH. TA also shifts
400   with salinity in winter, and at this location the DIC:TA ratio remains nearly constant along the salinity gradient (Fig. 4, Simpson
et al. 2022), which keeps pH similar.

Mid-layer pH

Winter median pH in the mid-layer is similar across nearshore sites (7.7) (Fig. 3a) and is slightly higher in the open waters of
405   the SOG (7.8). Winter mid-layer median pH is nearly the same as the surface median at all sites when the water column is
weakly stratified. Nearshore winter pH variability in the mid-layer is low compared to the surface, especially at Sansum
Narrows and Baynes Sound where the range is ~0.1. Summer mid-layer pH variability is similar to the range found in the
surface, and generally, medians are much lower than in the surface layer, when conditions are stratified and the surface is
productive. However, unlike other nearshore sites where summer surface pH is higher than in the mid-layer, median summer
410   mid-layer pH in Sansum Narrows is about the same (slightly lower, 0.05) than surface pH. Sansum Narrows also has the lowest
summer median mid-layer pH of the nearshore sites of 7.8, which is similar to the SOG.

3.1.5 Aragonite Saturation State – Ω_a

Surface Ω_a

Winter surface Ω_a are lower than summer Ω_a. Almost all nearshore locations and the SOG are completely undersaturated in
415 Ω_a in winter (Fig. 2b), with only a few outlying samples that are supersaturated. Median surface winter Ω_a is similar across all
sites (~0.8). In our data, the highest winter median Ω_a is found at the Evening Cove beach site (~0.9), and the lowest is found
in Baynes Sound (0.7). Winter surface variability in Ω_a is comparatively low relative to summer, ranging by ~ 0.5 at all
nearshore locations.

420 Summer Ω_a is high at our nearshore locations, which are mostly supersaturated and reach values as high as 3.2 (Okeover and
Baynes Sound). However, there is some summer surface undersaturation in Sansum Narrows and in the SOG. Median Ω_a at
nearshore locations is generally much higher (2.0 to 2.9) than in the SOG (1.6), except for in Sansum Narrows which has a
lower median Ω_a than the SOG. High Ω_a in Okeover Inlet stands out from other nearshore locations, and the highest median
Ω_a are found at Okeover beach and Okeover Inlet (2.9 and 2.8 respectively). The highest Ω_a values are also found in Okeover
425 Inlet, which are almost always greater than 2. There is large variability in Ω_a in summer across nearshore sites and the SOG
region, ranging by ~ 2. However, variability is lower in Sansum Narrows where the Ω_a range is only ~1.

Mid-layer Ω_a

430 Mid-layer Ω_a is similar to surface Ω_a in winter, with complete undersaturation at the nearshore and low variability (Fig. 3b).
SOG Ω_a is slightly higher than the nearshore and there is some supersaturation. Summer mid-layer Ω_a are lower than in the
surface, when the system is stratified and productive. Summer median mid-layer Ω_a are higher than in winter and similar across
nearshore sites, ~1.3, which is typically much lower than the surface medians, which range from 2.0 to 2.9. However, mid-
layer and surface median summer Ω_a in the SOG and Sansum Narrows are similar. Variability in the mid-layer is similar to
435 the surface, with variability being higher in Okeover Inlet and Baynes Sound, and lower in Sansum Narrows and the SOG.

3.1.6 Calcite Saturation State - Ω_c

Surface Ωc

Surface Ω_a and Ω_c follow a similar variability pattern although their values differ (i.e., Ω_c is greater). Winter Ω_c values and
variability are lower than in summer, and there is even some Ω_c undersaturation in winter at nearshore sites, particularly at
440 Baynes Sound and Okeover Inlet (Fig. 2c). The beach sites (Okeover and Evening Cove) are the only nearshore locations that
do not experience any Ω_c undersaturation in winter in our data. The SOG appears completely supersaturated in winter and
except for at the beaches, nearshore winter Ω_c are typically lower than in the SOG. Median winter surface Ω_c are similar across
all sites and are slightly greater than the saturation threshold, sitting just above 1.

445 In summer, Ω_c is supersaturated at all locations, and values and variability are much higher than in winter (Fig. 2c), with
maximum values reaching ~ 4.5 to 5.0. Nearshore sites typically have higher median Ω_c (3.4 to 4.6) than the SOG (~2.5), with

the exception of Sansum Narrows which has a similar median to the SOG and the lowest maximum values of all sites ~ 3. Summer variability in Ω_c is high across all sites, ranging by ~ 3.0 to 3.5 in the SOG, Baynes Sound and Evening Cove beach. Variability is lower in Okeover and Sansum Narrows, where Ω_c ranges by ~2.

450

Mid-layer Ωc

Winter mid-layer Ω_c are similar to winter surface Ω_c, with low values and low variability (Fig. 3c). All nearshore sites are mostly supersaturated, and the SOG is supersaturated throughout. Mid-layer median winter Ω_c are similar across nearshore
455 sites (~ 1.1), and median winter Ω_c in the SOG is slightly higher than in the nearshore (~1.5). Summer mid-layer Ω_c are higher than in winter across all nearshore locations. Summer median Ω_c are similar in the mid-layer across all nearshore sites, ~2, which is much lower than the surface medians at all sites except for Sansum Narrows, where surface and mid-layer medians are similar. Nearshore summer Ω_c variability in the mid-layer is similar to the surface, whereas variability in the SOG is lower in the mid-layer than in the surface.

460 **3.2 Drivers of Seasonal Change in pH and Ω**

Large changes in pH and Ω occur from winter to summer at all nearshore sites (Figs. 2 and 3, Table 2). The largest seasonal differences in pH and Ω are seen throughout Okeover Inlet, at beaches, and at the surface of Baynes Sound (Table 2, Fig. 5). Biologically driven changes in DIC ($\Delta DIC_{\bar{s}}$) contribute the most to seasonal change in pH and Ω, followed by seasonal ΔT (Fig. 5, Table A9). The temperature contribution to seasonal ΔpH is, however, much smaller than, and in the opposite direction
465 to, the contribution of $\Delta DIC_{\bar{s}}$ (15–20% of $\frac{\partial pH}{\partial DIC}\Delta DIC_{\bar{s}}$). The T contribution to seasonal change in Ω is negligible, 1– 2 orders of magnitude less than the contribution of $\Delta DIC_{\bar{s}}$ and is within, or close to, uncertainty.

Values of $\Delta TA_{\bar{s}}$ are all within or close to measurement uncertainty (Table 2) indicating no, or minimal, biologically mediated TA flux. Regardless, we estimated the magnitude of pH change that these relatively small $\Delta TA_{\bar{s}}$ would drive. Once errors are
470 **propagated through the Taylor analysis (see A3 for methods), there are two instances where the contribution of biological TA to seasonal change in pH is just greater than uncertainty (**

Table A9). These $TA_{\bar{s}}$ contributions to pH change drive a 0.05 (+/- 0.04) and 0.07 (+/-0.05) increase in pH from winter to summer, in the mid-layer at Baynes Sound and Okeover, respectively. These TA driven increases in pH indicate that there could be a small biological uptake of TA from the water in winter and/or a small biological TA source in summer, both of which seem unlikely. For a biological source of TA to be present in summer, dissolution of $CaCO_3$ structures would need to occur during times of Ω_a and Ω_c supersaturation. Equally, a TA sink in winter is unlikely due to widespread and persistent undersaturation. Changes in pH driven by in $TA_{\bar{s}}$ are negligible in relation to the contributions of $\Delta DIC_{\bar{s}}$ and ΔT and are of the same order of magnitude as uncertainty. Changes in Ω_a and Ω_c driven by $TA_{\bar{s}}$ are also low, close to uncertainty and negligible in relation to the contributions of $\Delta DIC_{\bar{s}}$ and ΔT.

The contributions of freshwater to seasonal changes in pH and Ω are also statistically negligible, as they are within or close to uncertainty, and any contribution outside of uncertainty is more than an order of magnitude less than the contribution from $\Delta DIC_{\bar{s}}$. Our results and discussion therefore focus on the contributions of $\Delta DIC_{\bar{s}}$ and ΔT to seasonal changes in pH, Ω_a and Ω_c.
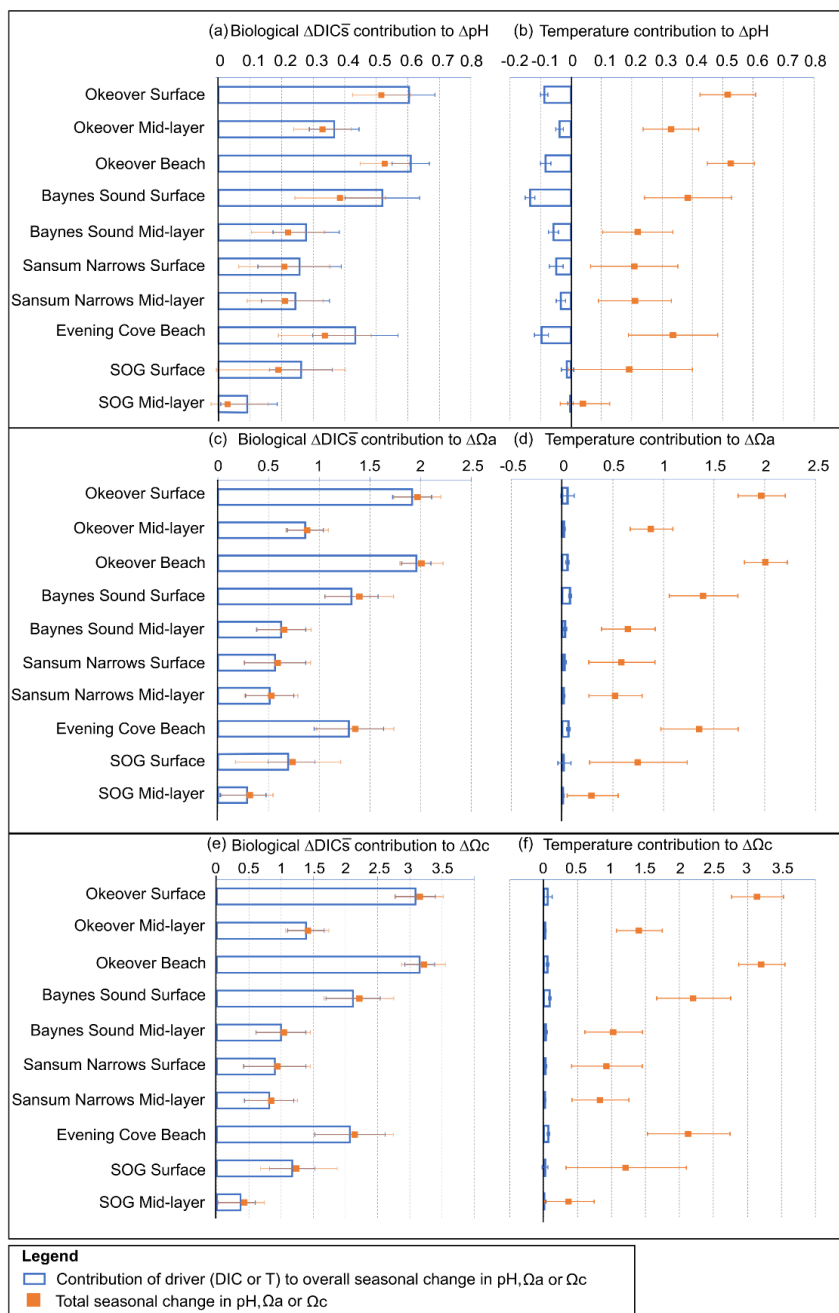
485

Figure 5. For each location, contribution of seasonal (winter to summer) biologically driven change in DIC (DICs) (left column) and seasonal temperature change, (right column) to seasonal change in pH (a,b), Ω_a (c,d) and Ω_c (e,f) (blue bars), respectively. Total seasonal change in pH, Ω_a and Ω_c resulting from all contributing drivers is shown in orange on each panel for comparison. Error bars are estimated from combining uncertainty from measurement, seasonal averaging, and partial derivative calculations (A3).

490

Table 1 Seasonal differences (summer minus winter) in mean DIC, TA, salinity, temperature pH, Ωa and Ωc at each location at each location (Sect. 2.3). $\Delta DIC_{\bar{s}}$ and $\Delta TA_{\bar{s}}$ values are the difference between the salinity-normalised mean summer minus mean winter DIC and TA (Sect. 2.2). ΔS and ΔT are the difference between mean winter and summer salinity and temperature. Values in bold are greater than uncertainty.

	$\Delta DIC_{\bar{s}}$ (µmol kg^{-1})	$\Delta TA_{\bar{s}}$ (µmol kg^{-1})	ΔT (°C)	ΔS	ΔpH	$\Delta \Omega a$	$\Delta \Omega c$
Okeover Beach	**-210** (+/-13)	**17** (+/- 15)	**5.4** (+/-0.9)	**-1.2** (+/-0.7)	**0.53** (+/- 0.08)	**2.01** (+/- 0.21)	**3.2** (+/- 0.3)
Okeover Surface	**-207** (+/- 17)	6 (+/- 13)	**5.7** (+/-0.8)	**-0.8** (+/-0.4)	**0.52** (+/- 0.09)	**1.97** (+/- 0.23)	**3.1** (+/- 0.4)
Okeover Mid-layer	**-105** (+/-17)	**16** (+/- 13)	**2.5** (+/-0.8)	**-0.5** (+/-0.3)	**0.33** (+/- 0.09)	**0.88** (+/- 0.21)	**3.2** (+/- 0.3)
Baynes Sound Surface	**-151** (+/-22)	-12 (+/- 23)	**9** (+/-0.9)	1.2 (+/-1.0)	**0.39** (+/- 0.14)	**1.4** (+/- 0.3)	**2.2** (+/- 0.5)
Baynes Sound Mid-layer	**-79** (+/- 24)	**20** (+/-13)	**3.9** (+/-0.9)	**-0.71** (+/-0.19)	**0.22** (+/- 0.12)	**0.65** (+/- 0.27)	**1.0** (+/- 0.4)
Evening Cove Beach	**-140** (+/- 30)	-4 (+/- 17)	**6.5** (+/-1.5)	**-1.7** (+/-0.5)	**0.34** (+/- 0.15)	**1.4** (+/- 0.4)	**2.1** (+/- 0.6)
Sansum Narrows Surface	**-70** (+/- 30)	4 (+/-14)	**3.3** (+/-1.5)	-0.4 (+/-0.9)	**0.21** (+/- 0.14)	**0.6** (+/- 0.3)	**0.9** (+/- 0.5)
Samsun Narrows Mid-layer	**-70** (+/-30)	8 (+/-14)	**2.3** (+/-0.8)	**-1.1** (+/-0.3)	**0.21** (+/- 0.12)	**0.53** (+/- 0.26)	**0.8** (+/- 0.4)
SOG Surface	**-81** (+/-21)	-20 (+/- 30)	0.7 (+/-1.6)	-0.4 (+/-1.3)	0.19 (+/- 0.20)	**0.8** (+/- 0.6)	**1.2** (+/- 0.9)
SOG mid-layer	**-26** (+/-22)	2 (+/- 13)	-0.1 (+/-0.8)	-0.5 (+/-0.7)	0.04 (+/- 0.09)	0.23 (+/- 0.23)	0.4 (+/- 0.4)

495

3.2.1 Seasonal pH change

From winter to summer, a seasonal increase in pH is found across all sites (Fig. 5a, Table 2). The magnitude of the seasonal increase in pH ranges from 0.04 to 0.53 and varies by location and depth ranging from 0.04 to 0.53. Typically, the greatest seasonal changes are at the surface and at beach sites. Okeover Inlet stands apart from other locations as the largest seasonal increase in pH occurs at Okeover beach (0.53) and Okeover surface layer (0.52). Large seasonal pH differences are even seen in the mid-layer in Okeover Inlet (0.33), where seasonal pH change is the same (within uncertainty of each other) as Evening Cove beach (0.34) and in the surface of Baynes Sound (0.39). Seasonal pH change is lower in the surface at Sansum Narrows, which is the same as mid-layer change in Sansum Narrows and Baynes sound and the surface of the SOG (~0.2). Mid-layer seasonal pH changes are lower than at the surface at all sites and are especially low in the SOG (0.04).

The driver contributing the most to seasonal change in pH (ΔpH) is biologically driven change in DIC ($\Delta DIC_{\bar{s}}$), which contributes significantly more to ΔpH than any other driver (Fig. 5a,

Table 9). At all locations, $\Delta DIC_{\bar{s}}$ driven pH increase dwarfs contributions from other drivers. The largest ΔpH typically corresponds with the largest $\Delta DIC_{\bar{s}}$ (Table 1). Sensitivities of ΔpH to $\Delta DIC_{\bar{s}}$ are similar across all sites (Table A4) and therefore

515   do not appear to influence the regional differences observed in ΔpH (Fig. 5a,b).

The positive temperature change from winter to summer has little influence on seasonal ΔpH. It drives pH in the opposite direction to $\Delta DIC_{\bar{s}}$ (Fig. 5g), decreasing pH from winter to summer. The temperature driven ΔpH is an order of magnitude less than the biologically driven change (i.e from $\Delta DIC_{\bar{s}}$) (Fig. 5a,b). ΔT accounts for a larger proportion of surface ΔpH in

520   Baynes Sound and Evening Cove beach than at other locations, as the seasonal difference in temperature at these locations is larger. However, $\Delta DIC_{\bar{s}}$ still drives most ΔpH at these locations. Mid-layer ΔpH in Okeover Inlet appears large, even relative to the ΔpH in the surface at Baynes Sound and Evening Cove, despite having smaller $\Delta DIC_{\bar{s}}$ (Table 1), although uncertainty envelopes overlap. Larger seasonal ΔT at Baynes Sound and at Evening Cove could be driving pH in the opposite direction to $\Delta DIC_{\bar{s}}$, reducing the ΔpH at these locations.

525   **3.2.2 Seasonal change in CaCO₃ saturation states**

Saturation states of Ω_a and Ω_c also increase from winter to summer; and although the magnitudes of change are different, both Ω_a and Ω_c follow similar patterns of seasonal change (Fig. 5, Table 1). Seasonal changes in Ω also follow a similar pattern to pH. Sites with large seasonal pH increases also experience large seasonal Ω increases. The seasonal change in surface saturation states at nearshore locations is large and >1, bringing the almost completely undersaturated conditions (with respect

530   to aragonite) in winter into supersaturation in summer. The largest seasonal increases in Ω_a and Ω_c are found at Okeover beach and in the Okeover Inlet surface layer (~2 Ω_a and 3 Ω_c).

Typically, mid-layer seasonal Ω_a and Ω_c difference is less than in the surface, except for Sansum Narrows where it is similar; and the seasonal difference in both the surface and mid-layer Ω_a and Ω_c in Sansum Narrows is lower than at other nearshore

535   sites. Sansum Narrows also has lower surface seasonal change than the SOG. However, in our data, the lowest seasonal Ω_a and Ω_c changes are seen in the mid-layer of the SOG.

The driver contributing the most to seasonal changes in Ω_a and Ω_c is $\Delta DIC_{\bar{s}}$, which contributes an order of magnitude more than any other driver (Fig. 5c,e,

540

Table A9). At most locations, $\Delta DIC_{\bar{s}}$ change accounts for all of the seasonal variability in Ω_a and Ω_c. Temperature has less effect on seasonal change in Ω than it does on pH, and unlike pH, drives Ω in the same direction as $\Delta DIC_{\bar{s}}$, i.e., causing a further increase in Ω in summer. Like pH, the largest change in seasonal Ω typically correspond with the largest $\Delta DIC_{\bar{s}}$ (Table 1), and sensitivities of Ω_a and Ω_c to $\Delta DIC_{\bar{s}}$ are similar across all sites (Table A4).

545 3**.3 Daily Variability**

3.3.1 Temperature

Winter temperatures on the days that we investigated (Sect. 2.4) are similar across all three sites (8 to 9 °C) and there is little variability in temperature over the day (Fig. 4e, Table 2). Summer temperatures are much higher, reaching up to ~ 20 °C in Baynes Sound and at Evening Cove beach, and 22.5 °C at the Okeover beach. While Baynes Sound experiences little
550 temperature variability (<1° C) in summer, temperature varies by ~2 to 3 °C at the other nearshore locations. Sansum Narrows has the greatest variability in summer temperature and is cooler than the other locations by ~4 °C.

3.3.2 Salinity

Summer salinities are slightly fresher than winter and there is typically low diel variability in salinity in both seasons (Fig. 4d, Table 2). However, Baynes Sound experiences a large range in diel salinity on the winter day, spanning from 22 to 28. This
555 larger diel variability was driven by heavy rainfall during the week preceding our sampling (17th November 2017) which also reduced the median surface salinity to 22.5. Some summer diel variability is also detected in Sansum Narrows as salinity decreases from 28 to 26 over the day, as new water is brought in with tides.

3.3.3 DIC and TA

Winter DIC and TA are higher than summer at all locations and follow salinity. Winter variability is low at Sansum Narrows
560 and Evening Cove beach where the salinity range is low, but variability is high in Baynes Sound, following the large variability in salinity. Summer DIC (both absolute and salinity normalized) is much lower than in winter at all locations (Fig. 4 f,g), and variability in summer DIC is greater than in winter at most locations, as biological fluxes during this productive season decrease DIC into the afternoon. In contrast, we found almost no summer diel variability in DIC in Baynes Sound in our observations. Summer TA also follows salinity (Fig. d, 4 h) and there is typically no diel TA variability, and where there is, this diel change
565 throughout the day is either within or close to uncertainty (Table 2).

Summer TA and DIC in Okeover are the lowest of all the sites (Fig. 4). We investigate the summer day in Okeover during the unusual coccolithophore bloom (August 2016). TA has been drawn down as the coccolithophores take up and use CO_3^{2-} from the water to build their shells. The mean TA drawdown is approximately 140 µmol kg^{-1} compared to "typical summer"
570 conditions (at the same salinity), resulting in a reduction of -0.3 pH, -1.4 Ω_a and -2.2 Ω_c relative to typical summer conditions.

There appears to be no diel TA change on the day that we sampled, when the bloom was already well developed (Table 2). Diel DIC change during the coccolithophore bloom is lower than at other locations, but overall DIC is lower, and median DIC (~1550 µmol kg^{-1}) is similar to a "typical summer', indicating that DIC drawdown has already occurred on a longer temporal scale.

3.3.4 pH

In our observations, the maximum winter diel pH change is lower than in summer at all locations. Median winter pH is ~ 7.7 in Baynes Sound and Sansum Narrows but is slightly higher at Evening Cove beach (7.86). Winter diel pH variability is higher (~0.2 to 0.3) in Baynes Sound and Evening Cove beach than in Sansum Narrows. At the beach, winter pH increases throughout the morning into the afternoon, whereas winter pH in Baynes Sound does not increase over the day but fluctuates with salinity. In summer, pH is higher than winter reaching medians of ~ 8- 8.2. Summer pH variability is higher than winter at Evening Cove and Sansum Narrows but is lower in Baynes Sound.

3.3.5 Saturations states Ω_a and Ω_c

In winter, Ω are low, with complete Ω_a undersaturation throughout the day at Baynes Sound and Sansum Narrows. Evening Cove beach has higher Ω_a values in winter than other locations, with some supersaturation and a median ~1. In our observations, maximum winter diel Ω_a variability is low in Baynes Sound and Sansum Narrows, but up to ~ 0.6 at Evening Cove beach, as Ω_a increases over the course of the day. Winter Ω_c is also low but mostly supersaturated in Sansum Narrows and Evening Cove; however, some undersaturation occurs in Baynes Sound. Variability in Ω_c is similar to Ω_a, with low variability in Baynes Sound and Sansum Narrows, and greater variability at the beach.

Summer Ω_a are high, especially in Baynes Sound and at Evening Cove beach, where median values reach ~ 2.8. Sansum Narrows and Okeover beach have lower Ω_a than the other sites and are similar to each other (Ω_a median ~ 1.5 to 1.7 and a maximum Ω_a of ~2 to 2.5). In our observations at all locations, there is greater diel variability in Ω in summer as increases occur through the day. Summer Ω_c is also high, with higher values in Baynes Sound and at Evening Cove beach than in Sansum Narrows and Okeover beach. All sites are supersaturated with respect to Ω_c in summer, with values reaching as high as 5 at the Evening Cove beach.

Table 2 Maximum observed change in DIC, TA, salinity, temperature, pH and Ω over the course of a single day at each location (Sect. 2.4). $\Delta DIC_{\bar{s}}$ and $\Delta TA_{\bar{s}}$ values are determined from the difference between the earliest (morning), and latest (mid-afternoon) normalised DIC and TA recorded in the day. ΔS and ΔT are calculated as the difference between the earliest (morning), and latest (mid-afternoon) S and T. Values in bold are greater than uncertainty.

	Date	$\Delta DIC_{\bar{s}}$ (µmol kg^{-1})	$\Delta TA_{\bar{s}}$ (µmol kg^{-1})	ΔT (°C)	ΔS	ΔpH	$\Delta \Omega a$	$\Delta \Omega_c$
Baynes Sound Winter	17 Nov 2017	**26** **(+/- 8)**	**26** **(+/- 12)**	**-1.09** **(+/- 0.10)**	**-5.50** **(+/- 0.003)**	**0.08** **(+/- 0.06)**	**-0.18** **(+/-0.15)**	-0.23 (+/- 0.24)
Baynes Sound Summer	27 July 2016	-4 (+/-8)	10 (+/- 12)	0.92 (+/- 0.10)	**0.08** **(+/- 0.003)**	0.03 (+/- 0.05)	0.13 (+/-0.13)	0.21 (+/- 0.22)
Evening Cove Beach Winter	08 Feb 2016	**-25** **(+/-8)**	10 (+/- 12)	**0.78** **(+/- 0.10)**	**0.032** **(+/- 0.003)**	**0.09** **(+/- 0.05)**	**0.33** **(+/-0.14)**	**0.52** **(+/- 0.22)**
Evening Cove Beach Summer	14 Aug 2017	**-140** **(+/-8)**	-10 (+/- 12)	**2.91** **(+/- 0.10)**	**-0.092** **(+/- 0.003)**	**0.35** **(+/- 0.04)**	**1.20** **(+/-0.11)**	**1.90** **(+/- 0.18)**
Sansum Narrows Winter	09 Feb 2016	2 (+/- 8)	9 (+/- 12)	**0.26** **(+/- 0.10)**	**0.387** **(+/- 0.003)**	0.02 (+/-0.05)	0.07 (+/-0.12)	0.07 (+/- 0.19)
Sansum Narrows Summer	28 July 2016	**-132** **(+/- 8)**	**-28** **(+/- 12)**	**4.41** **(+/- 0.10)**	**-1.734** **(+/- 0.003)**	**0.32** **(+/- 0.04)**	**0.79** **(+/-0.10)**	**1.32** **(+/- 0.17)**
Okeover Beach Summer	26 Aug 2016	**-55** **(+/- 8)**	-12 (+/- 12)	**2.05** **(+/- 0.10)**	**-0.035** **(+/- 0.003)**	**0.85** **(+/- 0.04)**	**0.41** **(+/-0.14)**	**0.66** **(+/- 0.22)**

3.4 Drivers of Diel Change in Carbonate Chemistry

3.4.1 Winter

Winter diel pH and Ω changes are small, mostly driven by small contributions form from biologically driven change in DIC ($\Delta DIC_{\bar{s}}$) (Table A10). Primary production is low in winter and therefore smaller $\Delta DIC_{\bar{s}}$ drives small diel ΔpH or ΔΩ at all three sites (Table 2). Biological TA contribution ($\Delta TA_{\bar{s}}$) to diel ΔpH and ΔΩ in winter is most often negligible (i.e., within uncertainty). Freshwater and diel ΔT are both negligible drivers of diel ΔpH and ΔΩ at all sites in winter. There are no detectable diel ΔpH and ΔΩ in Sansum Narrows in winter, but some small diel changes (beyond but close to uncertainty) are detected in Baynes Sound and at Evening Cove beach. Small increases in pH (0.09 +/- 0.05), Ω_a (~0.3 +/- 0.14) and Ω_c (~0.5 +/- 0.22) are detectable at Evening Cove beach in winter, driven by biological drawdown of DIC, as the calm, clear day progressed (Table A10).

In Baynes Sound, a small pH increase of 0.08 (+/- 0.06) is detected over the winter day. The estimated ΔpH from $\Delta DIC_{\bar{s}}$ on this day is negative (-0.09 +/- 0.03), suggesting that a small amount of remineralization may have occurred. At most locations

620    $\Delta TA_{\bar{s}}$ and freshwater are negligible drivers of carbonate parameters (Table A10). However, on the winter day in Baynes Sound, a diel $TA_{\bar{s}}$ increase (~26 µmol kg^{-1}) increases pH by 0.09 (+/- 0.05), countering the decrease driven by $\Delta DIC_{\bar{s}}$. This TA increase also drives an increase in saturation states of 0.24 (+/- 0.12) Ω_a and 0.38 (+/- 0.19) Ω_c. A small freshwater contribution is also detected at Baynes Sound, where a decrease in salinity of ~ 5 over the day, contributes to a 0.07 (+/- 0.014) increase in pH and 0.2 (+/- 0.02) decrease in both Ω_a and Ω_c, however, the diel changes in Ω_a and Ω_c in winter at Baynes Sound are

625   essentially negligible (i.e. less than or close to uncertainty) (Table 2).

3.4.2 Summer

Like seasonal change, the main contributing driver of diel pH and Ω changes is biologically driven change in DIC ($\Delta DIC_{\bar{s}}$)(Table A10). Typically, large diel changes in pH, Ω_a and Ω_c occur over the day in summer driven primarily by biological DIC drawdown, although there is no detectable pH or Ω change in Baynes Sound in summer (Table 2). Temperature

630   and freshwater have negligible driving effects, and biological $TA_{\bar{s}}$ contributions are only detected at Sansum Narrows. The largest pH increase over the day in summer is observed at Evening Cove beach (0.35 +/- 0.04), followed by Sansum Narrows (0.32 +/- 0.04), and Okeover Inlet (0.85 +/-0.04) (Table 2). Changes in pH driven by $\Delta DIC_{\bar{s}}$ are ~0.4 (+/- 0.016), ~0.5 (+/- 0.011) and ~0.2 (+/- 0.018) at Evening Cove, Sansum Narrows, and Okeover, respectively (Table A10). The largest diel Ω_a increase is also observed at Evening Cove beach, followed by Sansum Narrows and Okeover Inlet, where $\Delta DIC_{\bar{s}}$ contributes

635   to an increase in Ω_a of ~ 1.3 (+/- 0.011), ~1 (+/- 0.05) and ~0.5 (+/-0.07), respectively.

Summer temperature increase over the day is the second largest driver of pH, driving a diel decrease in pH at all sites (Table A10). However, this temperature driven pH decrease is dwarfed by biological DIC and is less than 0.1 at all sites. Temperature also has a negligible driving effect on saturation states, increasing saturation states no more than 0.04.

640

Biological $TA_{\bar{s}}$ contributions to diel summer pH and Ω change are mostly within uncertainty (Table A10). However, at Sansum Narrows, a small $TA_{\bar{s}}$ decrease of 28 µmol kg^{-1} contributes to a decline in diel pH of -0.1 (+/- 0.04) and a decrease in Ω_a of 0.2 (+/- 0.09) and -0.4 (+/- 0.2) Ω_c, which could indicate uptake of $CaCO_3$ by calcifiers at this site, although small, is detectable. There is no detectable change in TA or TA driven change in pH or Ω during the summer day in Okeover, during the

645   coccolithophore bloom.

4. Discussion

4.1 Variability

650 At the nearshore locations, variability in pH and Ω is low in winter and high in summer. High summer variability is due to strong variability in primary production on the synoptic scale, as blooms come and go (e.g., Moore-Maley et al., 2016). When we sampled, we typically captured a different phase of a phytoplankton bloom during each campaign. On a diel scale, in summer, primary production drives pH and Ω up during the daylight hours, while respiration during the dark hours decreases
655 pH and Ω. In addition, variable weather conditions on different sampling days also result in variability in primary production. For example, light may either limit (e.g., overcast, windy) or enable phytoplankton (e.g., sunny, calm). Wind-mixing, following a period in which nutrients were limiting and carbon was drawn down, may provide nutrients and carbon to the surface, resulting in a brief, rapid reduction in pH (Moore-Maley et al., 2017) before stimulating a new bloom (Allen and Wolfe, 2013; Moore-Maley et al., 2016). As primary production is the major driver of higher pH and Ω, low variability in winter is a result
660 of lower primary production, due to phytoplankton growth being light-limited (Harrison, 1983; Allen and Wolfe, 2013).

4.2 Drivers of pH and Ω

4.2.1 $DIC_{\bar{s}}$ and $TA_{\bar{s}}$

The dominant driver of seasonal and diel pH and Ω changes in the Salish Sea is biologically driven DIC change ($\Delta DIC_{\bar{s}}$), which contributes an order of magnitude more to seasonal and diel ΔpH and ΔΩ than any other driver. At our locations, $\Delta DIC_{\bar{s}}$ is
665 caused by the consumption of carbon by primary production in spring-summer, which greatly outweighs any remineralisation signal. Drawdown of DIC occurs during periods of high oxygen saturation, indicating that DIC is drawn down by primary production (Fig. A1). While low light limits primary production in winter, strong spring-summer blooms are triggered when this light limitation is lifted (Harrison, 1983; Allen and Wolfe, 2013), resulting in the large seasonal differences in DIC, pH and Ω observed at the surface.

670

Seasonal variability in pH and Ω is higher in the surface layer (0 to 5 m) than the mid-layer (5 to 20 m) at all locations because of greater spring-summer production and the resulting, large $\Delta DIC_{\bar{s}}$ in the surface. Our study locations are highly stratified, with a fresher, less dense, surface layer which extends to ~ 5 m depth. Stratification limits mixing and holds phytoplankton in the photic zone of the surface layer, which prevents light limitation and results in large drawdown of DIC at the surface. The
675 effects of this primary production are observed in the summer diel results, where DIC drawdown throughout the day results in a diel pH and Ω increase. Although seasonal and diel changes are less prominent than in the surface, variability in pH and Ω are still observed in the more light-limited mid-layer. Spring-summer pH and Ω in the mid-layer are not as elevated as in the surface, but are higher in summer, as mid-layer waters mix with the DIC depleted and high pH and Ω waters of the surface layer.

680

Biological modulation of DIC is the major driver of pH and Ω change in the Salish Sea, as the region is highly sensitive to changes in DIC (Simpson et al., 2022; Jarníková et al., 2022). The Salish Sea region is sensitive as it is carbon rich (Ianson et al., 2016), due to long sub-surface residence times (Masson, 2002; Pawlowicz et al., 2007) that allow remineralized DIC to accumulate. TA is also relatively high, and DIC:TA ratios are close to 1, which places the Salish Sea in highly sensitive
685   carbonate space (Simpson et al., 2022, Moore-Maley et al., 2018). Processes that modulate the high DIC content in this sensitive system are therefore the main contributing drivers of pH and Ω change in the Salish Sea. Partial derivatives of pH and Ω (with respect to DIC) across locations were similar, indicating little variability in this high sensitivity throughout the Salish Sea (Table A4). The largest seasonal and diel ΔpH and $\Delta\Omega$ were found where the greatest $\Delta DIC_{\bar{s}}$ occurred. The magnitude of $\Delta DIC_{\bar{s}}$ (i.e., how productive a system is), rather than sensitivity, is therefore responsible for the difference in pH
690   and Ω variability observed at different nearshore locations on both diel and seasonal scales.

As the magnitude of DIC drawdown by primary production in spring-summer is key to driving high pH and Ω conditions which are favourable to calcifiers, any future changes to phytoplankton abundance or assemblage would likely have strong implications for OA in this region. Increased temperatures since 1999 have been linked to increased stratification and a
695   reduction in nutrient renewal in the surface ocean on a global scale, which in turn has reduced global primary production (Behrenfeld, et al. 2006). Regionally, the ~4°C temperature anomaly known as to the "Pacific Blob" event, reduced primary production in the coastal waters outside of the Salish Sea (Peña et al., 2018). Higher temperatures projected to occur with climate change could therefore limit the seasonal modulation of low to high pH and Ω in winter to summer by primary production in the already stratified Salish Sea, prolonging low pH and Ω undersaturation conditions.

700

Biologically driven changes in TA from biomineralization of $CaCO_3$ or dissolution of shells, could also drive large changes in pH and Ω due to the high sensitivity of the system, if they were greater. These fluxes ($\Delta TA_{\bar{s}}$) in our study, if present, are too small to detect and likely do not drive changes in pH or Ω in our system. In the future, biologically driven TA changes could become a more important driver of seasonal change in summer, as increased temperatures increase the likelihood of calcifying
705   coccolithophore blooms (Rivero-Calle et al., 2015; Harada et al., 2012). The coccolithophore bloom captured in 2016 was the only recorded bloom of this type, which occurred during particularly warm conditions. Although it had no effect on a diel scale, the coccolithophore bloom did have an impact on pH and Ω (reduction in pH by -1.4, and Ω_a by -2.2) compared to a "typical" summer.

4.2.2 Temperature

710   In our region, temperature drives relatively small changes in carbonate parameters relative to the large variability driven by DIC. Warming decreases pH and therefore counters the effect of DIC drawdown on pH on both seasonal and diel time scales, but has little direct influence on Ω. Although it is the second largest driver, the contribution of seasonal temperature change is

small at all locations, and pH changes resulting from this seasonal temperature difference are low (mostly <0.1). Where diel temperature changes in summer are relatively high (i.e., Sansum Narrows), the temperature contribution to pH decrease still remains <0.1. Temperature, therefore, is not a notable driver of diel or seasonal changes in pH and Ω in this region as it is dwarfed by the biological fluxes of DIC.

4.2.3 Freshwater

Freshwater influence is a negligible driver of pH and Ω change at nearshore locations in the Salish Sea, despite strong salinity gradients and the strong salinity control of both DIC and TA in the region (Ianson et al., 2016; Simpson et al. 2022). The SOG is characterised by estuarine circulation (LeBlond, 1983), with a relatively fresh surface layer that receives large riverine inputs primarily from the Fraser River (Moore-Maley et al., 2018), and a multitude of other, mainly pluvial rivers (Morrison et al., 2011). The large spring-summer input of freshwater received from the glacial freshet appears balanced by the large pluvial inputs in fall and winter when this region receives heavy rainfall. As a result, there is little change in salinity between seasons (typically a decrease between 0.4 - 1.7 from winter to summer), which is too minor to drive seasonal change in pH or Ω.

Where larger salinity changes occur (e.g., during significant rain events on a diel scale, such as in Baynes Sound in winter), changes in pH and Ω are driven by the ΔS being large enough to shift carbonate system constants. DIC and TA change driven by ΔS have negligible driving effects on pH and Ω as both DIC and TA shift together. In the Salish Sea, TA and DIC mixing lines run almost parallel to one another (Simpson et al., 2022), so shifting DIC and TA in response to ΔS keep the DIC:TA ratio similar, and thus pH and Ω remain similar. In other words, changing DIC and TA resulting from salinity changes shift pH and Ω in almost equal and opposite directions in this region, resulting in only minor changes in pH and Ω (Tables A9, A10). These minor changes are negligible in relation to biologically driven DIC change.

Despite being a minor driver in the Salish Sea, salinity determines the sensitivity of the system to changing DIC. Freshwater input and salinity change are important as they determine the magnitude of the effect of the major driver, $\Delta DIC_{\bar{s}}$, on ΔpH and $\Delta\Omega$. The Salish Sea is highly sensitive throughout, and thus ΔS does not change the sensitivity significantly (Simpson et al., 2022; Jarníková et al., 2022). In other estuarine environments, where DIC and TA mixing lines do not run parallel (e.g., Hu and Cai, 2013), freshwater induced salinity change could be a more significant driver. In these systems, carbonate system sensitivities to ΔDIC (e.g, βDIC) can significantly change as salinity decreases, resulting in larger ΔpH and $\Delta\Omega$ for the same change in DIC (Hu and Cai, 2013).

4.3 Variability and drivers at each location

4.3.1 Okeover Inlet

Okeover Inlet stands out from other nearshore locations as it has higher pH and Ω than other nearshore sites. This is especially true in summer due to higher primary production and is indicated by Okeover having some of the highest oxygen saturations of all nearshore locations in summer (Fig. A1). Okeover also has the greatest seasonal change in pH and Ω, driven by the largest seasonal $\Delta DIC_{\bar{s}}$ from primary production. Higher primary production is likely a result of Okeover Inlet containing high subsurface nutrients (Fig. A1) and experiencing frequent calm stratified conditions which prevent light limitation, and periodic wind-mixing of nutrient-rich water into the surface layer. Okeover Inlet is connected to the rest of the Salish Sea through the shallow and narrow Malaspina Inlet, which limits exchange of water between Okeover Inlet and the NSOG. This isolation of the Inlet results in nutrient trapping (e.g., Ianson et al., 2003), as long residence times allow for continued primary production, drawdown of DIC, and elevated pH and Ω in the surface in summer. High primary production at the surface contributes to concentrated nutrients in deeper waters from high organic rain, compounded by limited mixing with outside waters and a relatively small volume of water. This subsurface nutrient trapping can further enhance low pH and Ω at the surface, when these subsurface waters with high nutrient concentrations are mixed into the surface during wind events and stimulate primary production. In our observations, Okeover is also cooler than other locations in summer (with the exception of the coccolithophore bloom year), which may reduce the risk of temperature induced mortality of shellfish in this region as temperatures increase with climate change.

During the unusual coccolithophore bloom in Okeover Inlet in 2016 (NASA, 2016), TA was drawn down (in comparison to a "typical" summer) because of shell-building uptake of CO_3^{2-} by coccolithophores. However, there was no detectable biological drawdown of TA on a diel scale during this bloom, likely because bio-formation of $CaCO_3$ structures does not occur on diel times scales. Additionally, TA had likely already been drawn down over the beginning of the bloom prior to sampling. Diel $DIC_{\bar{s}}$ contribution to pH and Ω change during the coccolithophore bloom was lower than $DIC_{\bar{s}}$ contribution from "typical" phytoplankton assemblages at other nearshore sites. It is possible that the increase in turbidity from the coccolithophores (Secchi depth ~0.5 m in comparison to ~5.5 m during "typical" conditions) limited light required for primary production, and the bloom was already well developed. However, significantly more data from both typical and atypical blooms would be required to determine the differences in $\Delta DIC_{\bar{s}}$ with certainty.

4.3.2 Beach grow locations

Conditions at beach grow locations do not stand out from the surface layer of other nearshore locations, suggesting no clear advantage of a beach lease compared to a surface tray hang to shellfish growers. At Okeover and Evening Cove beaches, we did not observe any clear differences in terms of more elevated pH and Ω, greater variability, or greater seasonal change in carbonate chemistry, when compared with other nearshore locations. Primary production and associated DIC drawdown at the

beach sites are similar to that in the surface layer in other locations where shellfish are grown, indicated by similar $\Delta DIC_{\bar{s}}$ and oxygen saturation (Fig. A1). There were also no clear indications of pH elevation related to TA increase at the shell midden beach location in Okeover over other beaches or other nearshore sites.

780

Diel temperature increase at the beach locations was also similar to the surface layer at other sites. This similarity between shallow beach sites and the surface layer of other locations is likely a due to the surface layer also being shallow, (0 to 5 m deep), and a similar level of primary production throughout the nearshore. However, the highest median temperature was found at Evening Cove beach, ~ 4 °C higher than most locations. Given the association between shellfish mortality and high

785 temperatures (Wendling et al., 2014; King et al., 2019), as temperatures increase, shellfish farmers considering future grow locations may wish to choose a tray hang location rather than a beach grow site, to provide the option to drop trays deeper in the water column where temperatures are cooler to reduce heat stress.

4.3.3 Baynes Sound

Baynes Sound has the highest density of shellfish operations in the Salish Sea (Holden et al., 2019), high summer pH and Ω,

790 and large seasonal changes in surface pH and Ω driven by drawdown of DIC by primary production. The seasonal increase in pH and Ω driven by primary production is relatively high in Baynes Sound as it is continuously supplied with nutrients from the north (Olson et al., 2020) and from a deep SOG tidal injection from the south (Guyondet et al. 2022). Like Okeover Inlet, high nutrients provide conditions that enable primary production. However, in contrast to Okeover Inlet, Baynes Sound is not a nutrient trap, as it is well connected to the SOG and to a continual re-supply of nutrients, which prevents nutrient limitation

795 in the surface layer throughout spring-summer.

Despite high primary production driving strong seasonal changes, Baynes Sound is the only location to have minimal to no diel summer pH and Ω increase, and little to no biologically driven change in DIC over the day. The absence of diel pH or Ω increase in Baynes Sound might be explained by the number of commercially grown shellfish feeding on phytoplankton, which

800 could be reducing the standing stock of primary producers enough to reduce the local biological drawdown of DIC. A recent study has indicated that shellfish aquaculture in Baynes Sound is currently operating within the ecological carrying capacity and that cultured bivalves consume phytoplankton at a rate that reduces net production by up to ~30% in Deep Bay (Guyondet et al. 2022), which would decrease but not remove the diel ΔDIC. Our Baynes Sound site is relatively shallow (<20 m), and another explanation for the absence of diel changes could be that a respiration signal from the benthic zone is countering the

805 drawdown of DIC by primary production. However, neither a reduction in primary production nor a significant respiration signal appear likely, as oxygen saturation percentages are high even at the bottom of Baynes Sound (Fig. A1). As pH, Ω, and oxygen saturation remain high, another explanation for why a diel change is not observed in summer is that Baynes Sound is rapidly flushed with a residence time on the order of weeks (Guyondet et al. 2022). The rapid flushing of water masses could maintain stable DIC, pH, and Ω conditions at the location of sampling although primary production is still occurring.

810

4.3.4 Sansum Narrows

Strongly tidally mixed areas have low variability and lower seasonal change in pH and Ω. Sansum Narrows is characterised by rapid tidal streams flushing and mixing water through the narrow channels. As a result of this mixing, surface variability is similar to that found in the mid-layer, and much lower than the surface variability observed elsewhere. Nutrients are always

815 replete in Sansum Narrows as they are renewed at the surface by mixing (Fig. A1), enabling primary production which is the main driver of pH and Ω variability and seasonal change. The distinct differences between surface and mid-layer found at other locations are not observed at Sansum Narrows as the effect of DIC drawdown is diluted through a greater depth of the water column by mixing. Lower oxygen saturation at the surface in Sansum Narrows than at other locations (Fig. A1), indicates that phytoplankton are affected by light limitation as they (and the oxygen that they produce) are mixed down away from the

820 photic zone. As a result, pH and Ω do not become as elevated as other locations in summer, and Sansum Narrows has the lowest (but most steady) pH and Ω of the nearshore locations, which can sometimes be lower than the open waters of the SOG.

4.3.5 SOG

The open waters of the SOG appear to be as variable as the nearshore from our data but have lower summer pH and Ω than most nearshore sites and a smaller seasonal surface change in pH and Ω. The open waters of the SOG are not as productive in

825 the surface layer as the nearshore sites, as dense phytoplankton blooms are supported in the nearshore at times when blooms in the open waters are not. Weaker blooms in the open waters are likely more limited by greater mixing than in the nearshore. As a result, the surface SOG experiences a much smaller $\Delta DIC_{\bar{s}}$ and a smaller seasonal change in pH and Ω than in the nearshore.

5. Implications

830 The large seasonal and diel variability observed at the nearshore locations implies that shellfish are already exposed to large ranges and extremes of pH and Ω in the Salish Sea, including low pH and undersaturation of Ω_a, and even some undersaturation of Ω_c, in winter. The largest variability and seasonal changes in pH and Ω is found at the surface and at beaches where most commercially grown and wild shellfish are present. Although the open waters of the SOG are, like the nearshore, highly variable, pH and Ω are lower in the open waters than in the nearshore, and seasonal changes in pH and Ω are relatively small.

835

The large differences between the nearshore and the open waters of the SOG implies that ship-based data collection in open waters is not adequate for characterising and capturing the variability of carbonate chemistry and the extremes that vulnerable organisms experience at the nearshore. In addition, although numerical biogeochemical models are able to capture variability on a finer temporal scale than our observational data, even high-resolution models average spatially (e.g., Jarníková, et al.,

840 2022) or are built on open ocean data (e.g., Ekstrom et al., 2015) and are not likely to fully capture the high diel and seasonal

variability observed in the nearshore. High resolution models which are built upon locally collected nearshore data could provide a more accurate representation of the variability and conditions at locations where OA sensitive organisms are present; and also have the advantage of being able to interpolate between infrequent sample data.

845 DIC drawdown by primary production is the dominant driver of seasonal and diel pH and Ω change at nearshore locations and creates favourable conditions for shellfish in summer. Temperature, although important because of its link to shellfish disease, has a less important role with respect to the carbonate system. Temperature drives pH down from winter to summer but the effect is an order of magnitude smaller than for DIC. Temperature is therefore a minor driver of pH on seasonal and diel scales at the surface and at beach locations but has a negligible effect in the mid-layer. Temperature also has a negligible seasonal 850 and diel contribution to Ω change.

Although shellfish themselves do have the ability to alter the carbonate chemistry in their surrounding environment through shell building or dissolution, the resulting biological change in TA and associated change in pH and Ω are too small to detect. Even in dense shellfish aquaculture operations such as Baynes Sound, where aquaculture is significant enough to alter primary 855 production on a local scale (Guyondet et al., 2022), no detectable TA signal was observed.

Freshwater is a negligible driver of seasonal and diel changes in pH and Ω in temperate fjords, as summer glacial and winter pluvial freshwater inputs are similar. Salinity variability is a main control of variability in DIC and TA, but seasonal and diel change in salinity is not large enough to drive notable changes in pH and Ω. Salinity is however, still an important control of 860 pH and Ω sensitivities to DIC change, (e.g., Hu and Cai, 2013). Sensitivities across all our locations were high, but similar, as salinities at our locations were for the most part above the sensitive mid-salinity region.

Winter pH conditions in the Salish Sea are well below the present-day global average of 8.1 (Raven et al., 2005; Jiang et al., 2019) (i.e., 7.6 to 7.8) and Ω_a is persistently undersaturated. Although diel variability in winter may at times bring the beach 865 locations out of Ω_a undersaturation briefly, undersaturation of Ω_a persists in winter at most locations. Aragonite is primarily used by calcifying organisms to build shells at the early life stages (Waldbusser et al., 2015), and so this chronic winter Ω_a undersaturation is of significance to the timing of out-planting oyster seed. To avoid unfavourable Ω_a conditions, seed could be out-planted after the onset of the spring bloom when local surface conditions rapidly become supersaturated (Moore-Maley et al., 2016). Out-planting of vulnerable shellfish seed and juveniles is typically carried out in summer, avoiding stressful 870 conditions. At present, the summer shellfish growing period experiences high Ω_a greater than 1.5, which is favourable to shellfish growth (Waldbusser et al., 2015); and summer pH at our nearshore locations are above the present-day global averages.

Despite high pH and Ω_a, most shellfish mortality events recorded in the Salish Sea have occurred in summer (Cowan et al.,
875   2020; Morin et al., 2020) and not in winter when chronic undersaturation of Ω_a occurs, as well as some Ω_c undersaturation.
One possibility is that wild shellfish have become adapted to chronic exposure to lower Ω_a conditions, or that commercial
shellfish species are already tolerant to these winter conditions (e.g., Waldbusser et al., 2016). Additionally, values of Ω_c rather
than Ω_a are likely more relevant to shellfish during winter because juveniles are typically out-planted in summer and have
reached maturity and transitioned to calcite structures by winter. However, chronic exposure to stressful conditions in winter
880   could make shellfish more susceptible to disease during the subsequent summer season when temperatures rise. At present,
higher temperatures and disease appear to be a more immediate concern to shellfish growers in the Salish Sea than decreasing
pH and Ω (Morin et al., 2020).

As temperature is potentially a major cause of shellfish mortalities through stress and increased likelihood of disease (Wendling
885   et al., 2014; King et al., 2019), growers may wish to consider hanging shellfish, especially juveniles, deeper than the surface
layer in summer (e.g., Cassis et al., 2011). Temperatures in the mid-layer are cooler, and although pH tends to be slightly
lower, the mid-layer mostly remains supersaturated with respect to both Ω_a and Ω_c in summer. This strategy may reduce the
risk of disease and temperature induced mortality of shellfish, provided enough food is available. In addition, beaches do not
appear to have a clear advantage over tray hang sites in terms of carbonate chemistry. However, beach sites experience the
890   highest temperatures of all locations and may become less favourable locations in the future as temperature rises. Indeed,
extreme heat events have already caused mass mortalities of invertebrates in the inter-tidal areas of the Salish Sea (White et
al., 2021).

Conclusions

OA is projected to reduce pH and Ω in the coming decades, and the favourable summer conditions currently observed in the
895   Salish Sea may become less favourable, especially as pH and Ω in the Salish Sea are highly sensitive to DIC change (Jarníková
et al., 2022; Simpson et al., 2022). Some Ω_c undersaturation already occurs in winter, and these conditions will become more
common and widespread, increasing stress for adult shellfish in the winter season. The shift towards more stressful carbonate
conditions in winter, combined with higher temperatures in summer, could result in chronic exposure of calcifiers to stressful
environmental conditions. There is an opportunity for shellfish aquaculture operations and wild species management strategies
900   to adapt to these changing conditions. Highly productive areas such as Okeover Inlet may be preferable locations for shellfish
aquaculture tenures under OA, as these areas are likely less vulnerable to increasing acidification due to high primary
production. Well mixed locations such as Sansum Narrows might be less preferable, as pH and Ω are presently lower than at
other locations, and primary production is limited by mixing as phytoplankton are removed from the surface. Equally, beach
grow locations have the highest temperatures, and may be more susceptible to disease. Characterizing the conditions in the
905   nearshore environment and understanding their drivers is essential to understanding and adapting to the impacts of OA and
climate change.

910

Appendix A

A1 Endmembers

Table A1 Name and location of fresh and salty endmembers used for establishing the DIC-S and TA-S relationships used when normalising DIC and TA to annual S at each location (Fig. 1). See Simpson et al. (2022), A5 and text below for details on how the
915 **Cowichan River, Fraser River and SSOG endmembers were determined.**

Location	Fresh Endmember	Salty Endmember
Okeover	Tokenatch Creek	Okeover Deep
Okeover Beach	Tokenatch Creek	Okeover Deep
Sansum Narrows	Cowichan River	South SOG Mid-layer
Evening Cove Beach	Cowichan River	South SOG Mid-layer
Baynes Sound	Puntledge River	North SOG Mid-layer
SOG	Fraser River	Juan de Fuca Deep

Table A2 Endmember Chemical Properties: Salinity (S), Dissolved Inorganic Carbon (DIC), and Total Alkalinity (TA).

Endmember	S	DIC (μmol kg^{-1})	TA (μmol kg^{-1})	Source
Cowichan River	0.06	469	472	This document
Fraser River	0.06	958	955	This document
Juan de Fuca deep	33.9	2250	2264	Ianson et al., 2016
North SOG	29.7	2031	2045	Simpson et al., 2022
Okeover Deep	28.6	1936	1984	Simpson et al., 2022
Puntledge River	1.84	437	388	Simpson et al., 2022
South SOG	30.9	2083	2114	This document
Tokenatch Creek	0.06	170	116	Simpson et al., 2022

South Strait of Georgia Endmember

To define our South SOG (SSOG) endmember (the salty endmember for the Sansum Narrows and Evening Cove sites) we used ship collected data, collected between 2003-2012 from sampling stations in the SSOG and nearby waters (Stations 42, 46, 56, 59 in Ianson et al., 2016). The Sansum Narrows region is strongly mixed, as is incoming water from the SSOG, east of Satellite Channel from Haro Strait. Well mixed water from the SOG therefore likely enters Sansum Narrows at the 70 m sill of Satellite channel. We use an average of data from 75 – 250 m to define the salty endmember in Table A2 (e.g., Simpson et al, 2022). We also considered endmembers with shallower mixing depths closer to the sill depth of 75m; these fell on the same salinity- DIC and -TA relationship lines as our selected endmember, but were too fresh to capture all the salinity range in our observational data.

Fraser River Endmember

The Fraser River Endmember was determined from a single sample taken in New Westminster, BC, in March 2017.

Cowichan River Endmember

The Cowichan River is a large river with high discharge and is likely the most influential freshwater source throughout the Sansum Narrows area and at Evening Cove beach. We calculated DIC-S and TA-S relationships with several freshwater sources and the same SSOG salty endmember and assessed the fit of observational data to these relationships. We found that DIC-S and TA-S mixing-lines calculated from water properties of the Cowichan River and the SSOG salty endmember fit best with observations from Sansum Narrows and Evening Cove. The mean DIC and TA collected from the same upstream location of the Cowichan River were used for this fresh endmember.

A2 Partial derivative calculations

Partial derivatives were calculated at site specific mean annual salinity (Sect. 2.2, Table A3). Due to the large range in S present at each nearshore location and the strong control S has on the carbonate system, we use an annual mean S ($\overline{S}_{annual}$) that is location and depth specific, for our partial derivative calculations. We normalise all observational DIC and TA to the appropriate $\overline{S}_{annual}$, following Friis et al., 2003 (Sect. 2.2), to present typical conditions. Finally, for each location and depth, we solve the carbonate system, using the location and depth specific mean annual $DIC_{\overline{S}}$ and $TA_{\overline{S}}$, T, S and nutrients (Table A3), to yield the partial derivatives (Table A4).

Table A3 Values used to solve the carbonate system for partial derivative calculations.

Where $\bar{S}_{annual}$ is the annual mean salinity at the location and depth layer of interest, $\overline{DIC_s}$ and $\overline{TA_s}$ are the mean normalised
955   DIC and TA normalised to the location and depth specific $\bar{S}_{annual}$; and where $\bar{T}$, $\bar{Si}$ and $\overline{PO_4}$ are annual mean values
of temperature, silicic acid and phosphate, and $\bar{P}$ is mean pressure for the depth layer.

Location	$\bar{S}_{annual}$	$\overline{DIC_s}$ (µmol kg⁻¹)	$\overline{TA_s}$ (µmol kg⁻¹)	$\bar{T}$ (°C)	$\bar{Si}$ (µmol kg⁻¹)	$\overline{PO_4}$ (µmol kg⁻¹)	$\bar{P}$ (dbar)
Okeover Surface	26.2	1686	1834	11.3	37.9	4.5	2.5
Okeover Mid-layer	27.3	1813	1905	10.5	41.8	4.5	10.0
Okeover Beach	26.0	1686	1836	11.6	37.2	4.7	0.5
Baynes Sound Surface	25.9	1730	1831	12.9	41.4	1.4	2.5
Baynes Sound Mid-layer	28.2	1889	1968	11.3	44.4	1.9	10.0
Sansum Narrows Surface	28.2	1902	1977	11.2	41.7	1.8	2.5
Sansum Narrows Mid-layer	28.9	1946	2014	10.6	40.3	1.8	10.0
Evening Cove Beach	27.3	1813	1938	13.2	34.6	1.4	0.5
SOG Surface	26.8	1774	1898	11.2	32.9	1.2	2.5
SOG Mid-layer	27.6	1869	1945	10.6	38.8	1.6	10.0

Table A4 Partial derivatives by location and depth (annual mean) OIS – Okeover Inlet Surface, OIML – Okeover Inlet Mid-layer, OIB - Okeover Inlet Beach, BSS – Baynes Sound Surface, BSML – Baynes Sound Mid-layer, SNS – Sansum Narrows Surface, SNML – Sansum Narrows Mid-layer, ECB – Evening Cove Beach, SOGS – SOG Surface, SOGML – SOG Mid-layer.

	OIS	OIML	OIB	BSS	BSML	SNS	SNML	ECB	SOGS	SOGML
$\partial pH/\partial S$ (PSU^{-1})	-0.014	-0.013	-0.014	-0.013	-0.012	-0.012	-0.011	-0.013	-0.014	-0.012
$\partial \Omega a/\partial S$ (PSU^{-1})	-0.015	-0.008	-0.016	-0.010	-0.007	-0.006	-0.005	-0.013	-0.012	-0.006
$\partial \Omega c/\partial S$ (PSU^{-1})	-0.036	-0.020	-0.037	-0.025	-0.017	-0.016	-0.014	-0.030	-0.028	-0.017
$\partial pH/\partial T$ (°C^{-1})	-0.015	-0.015	-0.015	-0.015	-0.015	-0.015	-0.015	-0.015	-0.015	-0.015
$\partial \Omega a/\partial T$ (°C^{-1})	0.009	0.007	0.010	0.009	0.007	0.007	0.007	0.009	0.009	0.007
$\partial \Omega c/\partial T$ (°C^{-1})	0.010	0.009	0.010	0.010	0.009	0.009	0.009	0.011	0.010	0.009
$\partial pH/\partial DIC$ (µmol kg^{-1})$^{-1}$	-0.003	-0.003	-0.003	-0.003	-0.004	-0.004	-0.004	-0.003	-0.003	-0.004
$\partial \Omega a/\partial DIC$ (µmol kg^{-1})$^{-1}$	-0.009	-0.008	-0.009	-0.009	-0.008	-0.008	-0.008	-0.009	-0.009	-0.008
$\partial \Omega c/\partial DIC$ (µmol kg^{-1})$^{-1}$	-0.015	-0.013	-0.015	-0.014	-0.013	-0.012	-0.012	-0.014	-0.014	-0.013
$\partial pH/\partial TA$ (µmol kg^{-1})$^{-1}$	0.003	0.003	0.003	0.003	0.003	0.003	0.004	0.003	0.003	0.004
$\partial \Omega a/\partial TA$ (µmol kg^{-1})$^{-1}$	0.010	0.009	0.010	0.009	0.008	0.008	0.008	0.009	0.009	0.008
$\partial \Omega c/\partial TA$ (µmol kg^{-1})$^{-1}$	0.016	0.014	0.016	0.015	0.013	0.013	0.013	0.015	0.015	0.013

965

A3 Uncertainty in Taylor expansion results

While most previous ocean studies that use Taylor expansions do not consider uncertainty, our data cover exceptionally wide ranges in salinity and carbonate chemistry parameters (e.g., Fig. 2). Thus, we estimate the uncertainty in the contributions of each driving component, i.e., each term in a given expansion (eqs. 1-6). For example, consider the contribution of T to seasonal
970   variability in pH: we estimate the uncertainty of the partial derivative (∂pH/∂T) and the seasonal range (ΔT) (term 3 on the righthand side of eq.1). The uncertainty estimation for each driving component is discussed in detail the following subsection.

Partial derivative uncertainty

The partial derivatives used in the Taylor expansion are determined at annual mean conditions for each location. More
975   specifically, they are calculated at a mean salinity and temperature with $DIC_{\bar{s}}$ and $TA_{\bar{s}}$ (A2). We estimate the uncertainty in our derivatives from the uncertainty envelope of the seasonal change of each driving component. For example, we add or subtract the uncertainty in the seasonal change in T from the annual mean T and recalculate the derivatives (e.g., ∂pH/∂T).

Seasonal and diel change uncertainty

980 To calculate the uncertainty in the seasonal differences of driving components (e.g., ΔT), we took the geometric mean of uncertainty in mean summer conditions (standard error), mean winter conditions (standard error), and measurement uncertainty (pooled standard deviation of replicates, see Simpson et al., 2022) (Table A5, A6).

Freshwater term uncertainty

985 Uncertainty in the freshwater term (eqs. 4-6), was calculated from the uncertainty in ΔpH, $\Delta\Omega_a$ or $\Delta\Omega_c$ driven by seasonal or diel ΔS. The ranges in ΔDIC and ΔTA corresponding to the uncertainty envelope of ΔS (as above) were calculated, and ΔpH, $\Delta\Omega_a$ or $\Delta\Omega_c$ were recalculated with these DIC and TA ranges. For example, the seasonal ΔS at Okeover Beach was -1.2 +/- 0.7. We calculated the change in DIC and TA resulting from an increase and a decrease in S of 0.7. These DIC and TA pairs were then used to resolve the carbonate system, keeping all other parameters (except for S) the same. The resulting range in
990   pH, Ω_a and Ω_c is the freshwater uncertainty envelope for these parameters.

995

1000 **Table A5 Uncertainty in the seasonal mean DIC and TA for each location.**

Location	Summer DIC μmol kg⁻¹	Winter DIC μmol kg⁻¹	Total DIC μmol kg⁻¹	Summer TA μmol kg⁻¹	Winter TA μmol kg⁻¹	Total TA μmol kg⁻¹
Okeover Surface	11	4	15	2.9	2.8	6
Okeover Mid-layer	13	3	15	2.4	1.1	4
Okeover Beach	9	1.4	10	8	2.1	10
Baynes Sound Surface	15	7	21	11	8	19
Baynes Sound Mid-layer	18	4	23	2.6	1.2	4
Sansum Narrows Surface	20	8	29	5	2.8	8
Samsun Narrows Mid-layer	12	3	16	4	3	7
Evening Cove Beach	23	5	28	7	6	12
SOG Surface	25	8	20	17	16	30
SOG Mid-layer	9	11	20	4	9	13

1005

1010

1015

Table A6 Measurement uncertainty of DIC, TA, S and T.

Driver	Measurement uncertainty	Method / source
DIC	+/- 8 µmol kg^{-1}	95% credible interval (the second standard deviation) of the pooled standard deviations of replicate pairs for all campaigns, following Dickson (2007).
TA	+/- 12 µmol kg^{-1}	95% credible interval (the second standard deviation) of the pooled standard deviations of replicate pairs for all campaigns, following Dickson (2007).
S	+/- 0.01	Geometric mean of pooled standard deviations of replicate pairs for all campaigns.
T	+/- 0.5 °C	Castaway ™ instrument uncertainty

1020

1025

1030

1035 Table A7 Uncertainties in partial derivatives

	∂pH/ DIC	∂Ωa/∂DIC	∂Ωc/∂DIC	∂pH/∂TA	∂Ωa/∂TA	∂Ωa/∂TA
Okeover surface	+/-0.00016	+/-0.00017	+/-0.0003	+/-0.00007	+/-0.00008	+/-0.00013
Okeover mid-layer	+/-0.00019	+/-0.0004	+/-0.0006	+/-0.00006	+/-0.00010	+/-0.00016
Okeover beach	+/-0.00010	+/-0.00011	+/-0.00018	+/-0.00012	+/-0.00013	+/-0.00021
Baynes Sound surface	+/-0.00027	+/-0.0004	+/-0.0007	+/-0.00030	+/-0.0005	+/-0.0007
Baynes mid-layer	+/-0.00025	+/-0.0006	+/-0.0010	+/-0.00005	+/-0.00011	+/-0.00018
Evening Cove beach	+/-0.0003	+/-0.0008	+/-0.0013	+/-0.00011	+/-0.00024	+/-0.0004
Sansum Narrows surface	+/-0.00016	+/-0.0004	+/-0.0008	+/-0.00009	+/-0.00022	+/-0.0004
Sansum Narrows mid-layer	+/-0.0003	+/-0.0004	+/-0.0007	+/-0.00016	+/-0.00023	+/-0.0004
SOG surface	+/-0.0003	+/-0.0004	+/-0.0007	+/-0.0005	+/-0.0008	+/-0.0013
SOG mid-layer	+/-0.00022	+/-0.0007	+/-0.0010	+/-0.00018	+/-0.0004	+/-0.0007

	∂pH/ ∂T	∂Ωa/ ∂T	∂Ωc/ ∂S	∂pH/ ∂S	∂Ωa/ ∂S	∂Ωc/ ∂S
Okeover surface	+/-0.00008	+/-0.0004	+/-0.010	+/-0.00011	+/-0.00008	+/-0.0005
Okeover mid-layer	+/-0.00009	+/-0.0003	+/-0.0003	+/-0.00006	+/-0.000019	+/-0.00021
Okeover beach	+/-0.00008	+/-0.0004	+/-0.0004	+/-0.00020	+/-0.00014	+/-0.0009
Baynes Sound surface	+/-0.00009	+/-0.0003	+/-0.0003	+/-0.00027	+/-0.00010	+/-0.0009
Baynes mid-layer	+/-0.00009	+/-0.0003	+/-0.0003	+/-0.00004	+/-0.000011	+/-0.00013
Evening Cove beach	+/-0.00014	+/-0.0005	+/-0.0005	+/-0.0001	+/-0.00003	+/-0.0005
Sansum Narrows surface	+/-0.00010	+/-0.0003	+/-0.0003	+/-0.00004	+/-0.000012	+/-0.00016
Sansum Narrows mid-layer	+/-0.00016	+/-0.0007	+/-0.0007	+/-0.00012	+/-0.00006	+/-0.0005
SOG surface	+/-0.00018	+/-0.011	+/-0.019	+/-0.0004	+/-0.00020	+/-0.0016
SOG mid-layer	+/-0.00010	+/-0.009	+/-0.016	+/-0.00012	+/-0.00007	+/-0.0003

1040

1045

Table A8 Total number of samples taken at each location in the surface and mid layers.

Location	Number of samples
Okeover surface	99
Okeover mid-layer	75
Okeover beach	51
Baynes Sound surface	80
Baynes mid-layer	71
Evening Cove beach	46
Sansum Narrows surface	31
Sansum Narrows mid-layer	48
SOG surface	43
SOG mid-layer	67

Table A9 Seasonal Taylor expansion results. Contributions to total seasonal changes in pH, Ωa and Ωc from biological changes in DIC ($\frac{\partial pH}{\partial DIC}\Delta\text{DIC}_{\bar{s}}$) and TA ($\frac{\partial pH}{\partial TA}\Delta\text{TA}_{\bar{s}})$) , T ($\frac{\partial pH}{\partial T}\Delta T$), and freshwater ($\frac{\partial pH}{\partial fw}\Delta fw$).

	$\frac{\partial pH}{\partial DIC}\Delta\text{DIC}_{\bar{s}}$	$\frac{\partial pH}{\partial TA}\Delta\text{TA}_{\bar{s}}$	$\frac{\partial pH}{\partial T}\Delta T$	$\frac{\partial pH}{\partial fw}\Delta fw$
Okeover Surface	**0.60 (+/- 0.08)**	0.02 (+/- 0.04)	**-0.087 (+/-0.012)**	**0.009 (+/-0.006)**
Okeover 5-20m	**0.37 (+/- 0.08)**	**0.05 (+/- 0.04)**	**-0.037 (+/- 0.012)**	0.003 (+/-0.003)
Okeover Beach	**0.61 (+/- 0.06)**	0.05 (+/- 0.05)	**-0.083 (+/- 0.017)**	**0.016 (+/-0.011)**
Baynes Sound Surface	**0.52 (+/- 0.12)**	-0.04 (+/- 0.08)	**-0.134 (+/- 0.016)**	-0.015 (+/-0.014)
Baynes Sound 5-20m	**0.27 (+/- 0.11)**	**0.07 (+/- 0.05)**	**-0.057 (+/- 0.017)**	**0.0062 (+/-0.0023)**
Sansum Narrows Surface	**0.26 (+/- 0.13)**	0.01 (+/- 0.05)	**-0.048 (+/- 0.023)**	0.005 (+/-0.011)
Sansum Narrows 5-20m	**0.24 (+/- 0.11)**	0.03 (+/- 0.05)	**-0.032 (+/- 0.015)**	**0.011 (+/-0.003)**
Evening Cove Beach	**0.43 (+/- 0.12)**	-0.01 (+/- 0.05)	**-0.969 (+/- 0.023)**	**0.027 (+/-0.007)**
SOG Surface	**0.27 (+/- 0.09)**	-0.06 (+/- 0.12)	-0.021 (+/- 0.025)	**0.025 (+/-0.017)**
SOG 5-20m	**0.09 (+/- 0.08)**	-0.01 (+/- 0.06)	-0.001 (+/- 0.012)	**0.013 (+/-0.009)**
	$\frac{\partial \Omega a}{\partial DIC}\Delta\text{DIC}_{\bar{s}}$	$\frac{\partial \Omega a}{\partial TA}\Delta\text{TA}_{\bar{s}})$	$\frac{\partial \Omega a}{\partial T}\Delta T$	$\frac{\partial \Omega a}{\partial fw}\Delta fw$
Okeover Surface	**1.92 (+/- 0.19)**	0.05 (+/- 0.13)	**0.053 (+/-0.009)**	**-0.038 (+/-0.006)**
Okeover 5-20m	**0.86 (+/- 0.18)**	**0.14 (+/- 0.11)**	**0.019 (+/-0.011)**	**-0.021 (+/-0.0021)**
Okeover Beach	**1.96 (+/- 0.15)**	**0.17 (+/- 0.15)**	**0.051 (+/-0.016)**	**-0.055 (+/-0.012)**
Baynes Sound Surface	**1.32 (+/- 0.26)**	-0.11 (+/- 0.21)	**0.077 (+/-0.012)**	**0.040 (+/-0.011)**
Baynes Sound 5-20m	**0.62 (+/- 0.24)**	**0.17 (+/- 0.11)**	**0.029 (+/-0.014)**	**-0.024 (/-0.0013)**
Sansum Narrows Surface	**0.6 (+/- 0.3)**	0.04 (+/- 0.11)	**0.024 (+/-0.013)**	**-0.009 (+/-0.006)**
Sansum Narrows 5-20m	**0.51 (+/- 0.24)**	0.06 (+/- 0.11)	**0.029 (+/-0.009)**	**-0.025 (+/-0.0014)**
Evening Cove Beach	**1.3 (+/- 0.3)**	-0.04 (+/- 0.16)	**0.061 (+/-0.017)**	**-0.033 (+/-0.007)**
SOG Surface	**0.72 (+/- 0.23)**	-0.2 (+/- 0.3)	0.011 (+/-0.021)	**-0.013 (+/-0.006)**
SOG 5-20m	**0.20 (+/- 0.19)**	-0.02 (+/- 0.15)	0.004 (+/-0.006)	**-0.011 (+/-0.005)**
	$\frac{\partial \Omega c}{\partial DIC}\Delta\text{DIC}_{\bar{s}}$	$\frac{\partial \Omega c}{\partial TA}\Delta\text{TA}_{\bar{s}})$	$\frac{\partial \Omega c}{\partial T}\Delta T$	$\frac{\partial \Omega c}{\partial fw}\Delta fw$
Okeover Surface	**3.1 (+/- 0.3)**	0.09 (+/- 0.21)	0.06 (+/-0.06)	**-0.052 (+/-0.015)**
Okeover 5-20m	**1.38 (+/- 0.29)**	**0.22 (+/- 0.18)**	**0.022 (+/-0.012)**	**-0.031 (+/-0.006)**
Okeover Beach	**3.15 (+/- 0.23)**	**0.27 (+/- 0.25)**	**0.056 (+/-0.017)**	**-0.075 (+/-0.028)**
Baynes Sound Surface	**2.12 (+/- 0.26)**	-0.17 (+/- 0.34)	**0.089 (+/-0.014)**	**0.054 (+/-0.026)**
Baynes Sound 5-20m	**1.00 (+/- 0.24)**	**0.27 (+/- 0.17)**	**0.035 (+/-0.016)**	**-0.034 (+/-0.003)**
Sansum Narrows Surface	**0.9 (+/- 0.3)**	0.06 (+/- 0.19)	**0.028 (+/-0.015)**	-0.013 (+/-0.015)
Sansum Narrows 5-20m	**0.82 (+/- 0.24)**	0.10 (+/- 0.18)	**0.019 (+/-0.011)**	**-0.034 (+/-0.004)**
Evening Cove Beach	**2.1 (+/- 0.3)**	-0.06 (+/- 0.26)	**0.068 (+/-0.019)**	**-0.037 (+/-0.017)**
SOG Surface	**1.2 (+/- 0.2)**	-0.3 (+/- 0.5)	0.048 (+/-0.029)	-0.01 (+/-0.04)
SOG 5-20m	**0.32 (+/- 0.19)**	-0.03 (+/- 0.23)	**0.004 (+/-0.001)**	-0.012 (+/-0.013)

Table A10 Diel Taylor expansion results. Contributions to total diel changes in pH, Ωa and Ωc from biological changes in DIC ($\frac{\partial pH}{\partial DIC}\Delta DIC_{\bar{s}}$) and TA ($\frac{\partial pH}{\partial TA}\Delta TA_{\bar{s}}$), T ($\frac{\partial pH}{\partial T}\Delta T$), and freshwater ($\frac{\partial pH}{\partial fw}\Delta fw$).

	Date	$\frac{\partial pH}{\partial DIC}\Delta DIC_{\bar{s}}$	$\frac{\partial pH}{\partial TA}\Delta TA_{\bar{s}}$	$\frac{\partial pH}{\partial T}\Delta T$	$\frac{\partial pH}{\partial fw}\Delta fw$
Baynes Sound Winter	17-Nov-17	**-0.09 (+/- 0.03)**	**0.09 (+/- 0.05)**	**0.02 (+/- 0.01)**	**0.072 (+/- 0.014)**
Baynes Sound Summer	27-Jul-16	0.011 (+/- 0.027)	0.03 (+/- 0.04)	-0.01 (+/- 0.01)	0.001 (+/- 0.014)
Evening Cove Beach Winter	08-Feb-16	**0.082 (+/- 0.016)**	0.03 (+/- 0.04)	-0.01 (+/- 0.01)	-0.001 (+/- 0.014)
Evening Cove Beach Summer	14-Aug-17	**0.431 (+/- 0.016)**	-0.03 (+/- 0.03)	**-0.04 (+/- 0.01)**	0.002 (+/- 0.014)
Sansum Narrows Winter	09-Feb-16	-0.014 (+/- 0.029)	0.03 (+/- 0.04)	0.004 (+/- 0.01)	-0.004 (+/- 0.012)
Sansum Narrows Summer	28-Jul-16	**0.473 (+/- 0.011)**	**-0.10 (+/- 0.04)**	**-0.06 (+/- 0.01)**	**0.024 (+/- 0.012)**
Okeover Beach Summer	26-Aug-16	**0.162 (+/- 0.018)**	-0.03 (+/- 0.03)	**-0.03 (+/- 0.01)**	0.001 (+/- 0.015)
	Date	$\frac{\partial \Omega a}{\partial DIC}\Delta DIC_{\bar{s}}$	$\frac{\partial \Omega a}{\partial TA}\Delta TA_{\bar{s}}$)	$\frac{\partial \Omega a}{\partial T}\Delta T$	$\frac{\partial \Omega a}{\partial fw}\Delta fw$
Baynes Sound Winter	17-Nov-17	**-0.22 (+/- 0.08)**	**0.24 (+/- 0.12)**	**-0.011 (+/- 0.004)**	**-0.18 (+/- 0.022)**
Baynes Sound Summer	27-Jul-16	**0.03 (+/- 0.07)**	0.09 (+/- 0.11)	0.01 (+/- 0.01)	-0.003 (+/- 0.022)
Evening Cove Beach Winter	08-Feb-16	**0.22 (+/- 0.06)**	0.10 (+/- 0.12)	0.01 (+/- 0.01)	0.001 (+/- 0.008)
Evening Cove Beach Summer	14-Aug-17	**1.271 (+/- 0.011)**	-0.10 (+/- 0.11)	**0.03 (+/- 0.01)**	-0.002 (+/- 0.008)
Sansum Narrows Winter	09-Feb-16	-0.01 (+/- 0.07)	0.07 (+/- 0.10)	0.004 (+/- 0.01)	**0.012 (+/- 0.009)**
Sansum Narrows Summer	28-Jul-16	**1.03 (+/- 0.05)**	**-0.23 (+/- 0.09)**	**0.03 (+/- 0.01)**	**-0.044 (+/- 0.009)**
Okeover Beach Summer	26-Aug-16	**0.51 (+/- 0.07)**	-0.12 (+/- 0.12)	**0.02 (+/- 0.01)**	0.001 (+/- 0.016)
	Date	$\frac{\partial \Omega c}{\partial DIC}\Delta DIC_{\bar{s}}$	$\frac{\partial \Omega c}{\partial TA}\Delta TA_{\bar{s}}$)	$\frac{\partial \Omega c}{\partial T}\Delta T$	$\frac{\partial \Omega c}{\partial fw}\Delta fw$
Baynes Sound Winter	17-Nov-17	**-0.36 (+/- 0.13)**	**0.38 (+/- 0.19)**	**-0.012 (+/- 0.005)**	**-0.24 (+/- 0.03)**
Baynes Sound Summer	27-Jul-16	**0.05 (+/- 0.11)**	0.15 (+/- 0.18)	**0.011 (+/- 0.003)**	-0.004 (+/- 0.03)
Evening Cove Beach Winter	08-Feb-16	**0.36 (+/- 0.09)**	0.15 (+/- 0.19)	**0.012 (+/- 0.002)**	0.0011 (+/- 0.018)
Evening Cove Beach Summer	14-Aug-17	**2.032 (+/- 0.018)**	-0.16 (+/- 0.18)	**0.03 (+/- 0.002)**	-0.002 (+/- 0.018)
Sansum Narrows Winter	09-Feb-16	-0.02 (+/- 0.10)	0.11 (+/- 0.16)	0.001 (+/- 0.002)	0.012 (+/- 0.019)
Sansum Narrows Summer	28-Jul-16	**1.65 (+/- 0.07)**	**-0.37 (+/- 0.15)**	**0.04 (+/- 0.007)**	**-0.05 (+/- 0.019)**
Okeover Beach Summer	26-Aug-16	**0.83 (+/- 0.11)**	-0.19 (+/- 0.19)	**0.022 (+/- 0.006)**	-0.002 (+/- 0.04)

1055

1060
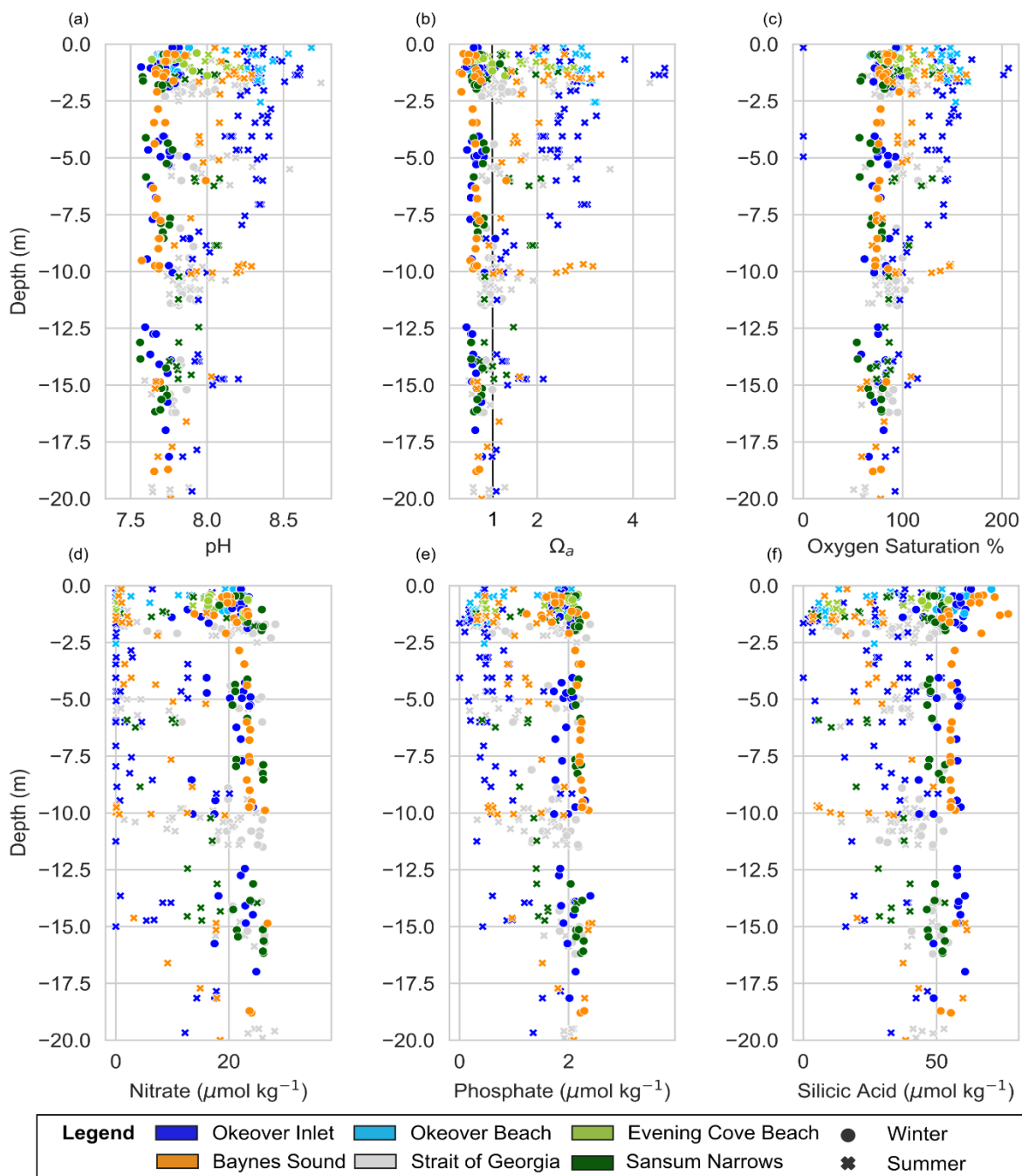
Figure A1. Winter (points) and summer (crosses) depth profiles of observational: a) pH, b) Ω$_a$, c) oxygen saturation, d) nitrate concentration, e) phosphate concentration, and f) silicic acid concentration, at each nearshore location and the SOG.

Data Availability

All data appear in figures and calculations are explicitly described. Raw data are archived within The National
Oceanic and Atmospheric Administration Ocean Carbon Data System, https://doi.org/10.25921/padc-s385.

Autor contribution

ES – conceptualization, data curation, formal analysis, investigation, methodology, project administration, software, visualization, writing – original draft preparation.

DI – conceptualization, methodology, investigation, funding acquisition, project administration, resources, supervision, validation, writing – review and editing.

KEK - conceptualization, methodology, investigation, funding acquisition, project administration, resources, supervision, validation, writing – review and editing.

AF –methodology, software, writing – review and editing.

PC – conceptualization, methodology, visualization, investigation, writing – review and editing.

MD – methodology, data curation, formal analysis, investigation, resources, supervision, validation, writing – review and editing.

YP – conceptualization, investigation, methodology, resources, writing – review and editing.

Competing Interests

The authors declare that they have no conflict of interest.

Acknowledgements

This work was funded by Marine Environmental Observation Prediction and Response Network Ocean Acidification in Canadian Coastal Communities: Project 2.9 An Integrated Coastal Acidification Program to KEK and DI. KEK was funded by National Science and Engineering Research Council Canada Research Chair Award. We thank Keith Reid and all at Stellar Bay Shellfish, who helped frame the goals of this research, and hosted and made time for us at their busy shellfish aquaculture lease. Sincere thanks also go Andrew Dryden and all at Evening Cove Oysters, for allowing us to sample at their private property, even at antisocial times of day, and for the time and resources used to take us between sampling locations during their workday. Warm thanks to Andre and Chris at Okeover Organic Oysters, for all their time, driving us between multiple sampling sites, aiding the search for lost equipment and for the fresh oysters. We thank Kenny Scozzafava, Mark Belton,

Tamara Fraser, Danielle Caleb for their help with sample collection and analysis. Carolyn Prentice, Aimee McGowan, Sergey Tsynkevych, Stephen Chastain, Michelle Vandermoor, Tyler Carlson, Amelia Hesketh, Ben Hudson, Tereza Jarníková, Elise Olson, Evie Morin, and Vancouver Island University Marine Field Station staff for help collecting samples.

References

1095 Alin, S. R., Brainard, R. E., Price, N. N., Newton, J. A., Cohen, A., Peterson, W. T., et al.: Characterizing the natural system: Toward sustained, integrated coastal ocean acidification observing networks to facilitate resource management and decision support, Oceanography, 28(2), 92-107, https://doi.org/10.5670/oceanog.2015.34, 2015.

Allen, S. E. and Wolfe, M. A.: Hindcast of the timing of the spring phytoplankton bloom in the Strait of Georgia, 1968-2010,
1100 Progress in Oceanography, 115, 6-13, https://doi.org/10.1016/j.pocean.2013.05.026, 2013.

Banas, N., Hickey, B., Newton, J., & Ruesink, J.: Tidal exchange, bivalve grazing, and patterns of primary production in Willapa Bay, Washington, USA, Marine Ecology Progress Series, 341, 123–139, https://doi.org/10.3354/meps341123, 2007.

1105 Barton, A., Hales, B., Waldbusser, G. G., Langdon, C., & Feely, R. A.: The Pacific oyster, Crassostrea gigas, shows negative correlation to naturally elevated carbon dioxide levels: Implications for near-term ocean acidification effects, Limnology and oceanography, 57 (3), 698–710, https://doi.org/10.4319/lo.2012.57.3.0698, 2012.

Barwell-Clarke, J. and Whitney, F.: Institute of Ocean Sciences Nutrient Methods and Analysis, Canadian Technical Report
1110 of Hydrography and Ocean Sciences, 182, 43, 1996.

Beaupre-Laperriere, A., Mucci, A., and Thomas, H.: The recent state and variability of the carbonate system of the Canadian Arctic Archipelago and adjacent basins in the context of Ocean Acidification, Biogeosciences, 17, 3923-3942, https://doi.org/10.5194/bg-17-3923-2020, 2020.
1115

Behrenfeld, M., O'Malley, R., Siegel, D. et al.: Climate-driven trends in contemporary ocean productivity, Nature, 444, 752-755, https://doi.org/10.1038/nature05317, 2006.

Cai, W. J., Hu, X., Huang, W. J., Murrell, M. C., Lehrter, J. C., Lohrenz, S. E., Chou, W. C., Zhai, W., Hollibaugh, J. T.,
1120 Wang, Y., Zhao, P., Guo, X., Gundersen, K., Dai, M., and Gong, G. C.: Acidification of subsurface coastal waters enhanced by eutrophication, Nature Geoscience, 4, 766-770, https://doi.org/10.1038/ngeo1297, 2011.

Cai, W. J., Feely, R. A., Testa, J. M., Li, M., Evans, W., Alin, S. R., et al.: Natural and anthropogenic drivers of acidification in large estuaries, Ann. Rev. Mar. Sci., 13, 23–55, https://doi.org/10.1146/annurev-marine-010419-011004, 2021.

1125

Cai, W. J., Xu, Y. Y., Feely, R. A., Wanninkhof, R., Jonsson, B., Alin, S. R., et al.: Controls on surface water carbonate chemistry along North American ocean margins, Nat. Comms., 11, 2691, https://doi.org/10.1038/s41467-020-16530-z, 2020.

Caldeira, K. and Wickett, M. E.: Anthropogenic carbon and ocean pH, Nature, 425, 365, https://doi.org/10.1038/425365a,
1130   2003.

Carpenter, J.H.: The Chesapeake Bay Institute Technique for the Winkler Dissolved Oxygen Method. Limmnol. & Oceanogr., 10, 141-143, 1965.

1135   Cassis, D., Pearce, C.M., Maldonado, M.T.: Effects of the environment and culture depth on growth and mortality in juvenile Pacific oysters in the Strait of Georgia, British Columbia, Aquacult. Environ. Interact. 1:259-274, https://doi.org/10.3354/aei00025, 2011.

Cooley, S. R., Lucey, N., Kite-Powell, H., and Doney, S. C.: Nutrition and income from molluscs today imply vulnerability to
1140   ocean acidification tomorrow, Fish Fish., 13, 182–215, https://doi.org/10.1111/j.1467-2979.2011.00424.x, 2012.

Cowan, M.: Exploring the mechanisms of Pacific oyster summer mortality in Baynes Sound aquaculture. MSc Thesis, University of Victoria, Victoria, British Columbia, 2020.

1145   Dickson, A. G.: Standard potential of the reaction: AgCl(s) + 1/2H2(g) = Ag(s) + HCl(aq), and the standard acidity constant of the ion HSO4- in synthetic seawater from 273.15 to 318.15 K. Journal of Chemical Thermodynamics, 22(2), 113-127. https://doi.org/10.1016/0021-9614(90)90074-Z, 1990.

Dickson, A. G., Sabine, C. L., & Christian, J. R. (Eds.): Guide to Best Practices for Ocean CO2 Measurements. PICES Special
1150   Publication 3, 191 pp. https://cdiac.ess-dive.lbl.gov/ftp/oceans/Handbook_2007/Guide_all_in_one.pdf; Chapter 4; SOP 3, 2007.

Dickson, A. G.: Guide to best practices for ocean acidification research and data reporting. In U. Riebesell, V. J. Fabry, L. Hansson, & J.-P. Gattuso (Eds.), (pp. 191-228). Luxembourg: Publications Office of the European Union, 2010.
1155

Doney, S. C., Mahowald, N., Lima, I., Feely, R. A., Mackenzie, F. T., Lamarque, J.-F., & Rasch, P. J.: Impact of anthropogenic atmospheric nitrogen and sulfur deposition on ocean acidification and the inorganic carbon system. Proceedings of the National Academy of Sciences, 104(37), 14580-14585. https://doi.org/10.1073/pnas.0702218104, 2007.

1160 Doney, S. C., Busch, D. S., Cooley, S. R., & Kroeker, K. J.: The impacts of ocean acidification on marine ecosystems and reliant human communities. Annual Review of Environment and Resources, 45, 83-112. https://doi.org/10.1146/annurev-environ-012320-083019, 2020.

Duarte, C. M., Hendriks, I. E., Moore, T. S., Olsen, Y. S., Steckbauer, A., Ramajo, L., et al.: Is ocean acidification an open-
1165 ocean syndrome? Understanding anthropogenic impacts on seawater pH. Estuaries and Coasts, 36(2), 221-236. https://doi.org/10.1007/s12237-013-9594-3, 2013.

Egleston, E. S., Sabine, C. L., & Morel, F. M. M.: Revelle revisited: Buffer factors that quantify the response of ocean chemistry to changes in DIC and alkalinity, Global Biogeochem. Cycles, 24(1), https://doi.org/10.1029/2008GB003407, 2010.
1170

Ekstrom, J. A., Suatoni, L., Cooley, S. R., Pendleton, L. H., Waldbusser, G. G., Cinner, J. E., et al.: Vulnerability and adaptation of US shellfisheries to ocean acidification, Nat. Clim. Change, 5(3), 207–214, https://doi.org/10.1038/nclimate2508, 2015.

Evans, W., Pocock, K., Hare, A., Weekes, C., Hales, B., Jackson, J., et al.: Marine CO2 patterns in the northern Salish Sea,
1175 Front. Mar. Sci., 5, 1–18, https://doi.org/10.3389/fmars.2018.00536, 2019.

Feely, R. A., Alin, S. R., Newton, J., Sabine, C. L., Warner, M., Devol, A., et al.: The combined effects of ocean acidification, mixing, and respiration on pH and carbonate saturation in an urbanized estuary, Estuar. Coast. Shelf Sci., 88(4), 442–449, https://doi.org/10.1016/j.ecss.2010.05.004, 2010.
1180

Fassbender, A. J., Alin, S. R., Feely, R. A., Sutton, A. J., Newton, J. A., Krembs, C., et al.: Seasonal carbonate chemistry variability in marine surface waters of the US Pacific Northwest, Earth Syst. Sci. Data, 10(3), 1367–1401, https://doi.org/10.5194/essd-10-1367-2018, 2018.

1185 Franco, A. C., Ianson, D., Ross, T., Hamme, R. C., Monahan, A. H., Christian, J. R., Davelaar, M., Johnson, W. K., Miller, L. A., Robert, M., and Tortell, P. D.: Anthropogenic and Climatic Contributions to Observed Carbon System Trends in the Northeast Pacific, Global Biogeochem. Cycles, 35, https://doi.org/10.1029/2020GB006829, 2021.

Friis, K., Körtzinger, A., and Wallace, D. W. R.: The salinity normalization of marine inorganic carbon chemistry data,
1190   Geophys. Res. Lett., 30, https://doi.org/10.1029/2002GL015898, 2003.

Gimenez, I., Waldbusser, G. G., & Hales, B.: Ocean acidification stress index for shellfish (OASIS): Linking Pacific oyster
larval survival and exposure to variable carbonate chemistry regimes, Elem., 6(1), https://doi.org/10.1525/elementa.306, 2018.

1195   Gruber, N., Clement, D., Carter, B. R., Feely, R. A., Van Heuven, S., Hoppema, M., et al.: The oceanic sink for anthropogenic
CO2 from 1994 to 2007, Science, 363(6432), 1193–1199. https://doi.org/10.1126/science.aau515, 2019.

Guyondet, T., Krassovski, M.V., Sutherland, T.F., Foreman, M.G.G., & Filgueira, R.: An ecological carrying capacity
assessment for shellfish aquaculture in Baynes Sound, British Columbia. Canadian Science Advisory Secretariat, Fisheries
1200   and Oceans Canada. https://publications.gc.ca/collections/collection_2022/mpo-dfo/fs70-5/Fs70-5-2022-003-eng.pdf, 2022.

Haigh, R., D. Ianson, C. A. Holt, H. E. Neate, and A. M. Edwards.: Effects of ocean acidification on temperate coastal marine
ecosystems and fisheries in the northeast Pacific. PLoS One, 10(2), e0117533. https://doi:10.1371/journal.pone.0117533,
2015.

1205
Harada, N., Sato, M., Oguri, K., Hagino, K., Okazaki, Y., Katsuki, K., et al.: Enhancement of Coccolithophorid Blooms in the
Bering Sea by Recent Environmental Changes. Global Biogeochemical Cycles, 26(2), https://doi:10.1029/2011GB004177,
2012.

1210   Hare, A., Evans, W., Pocock, K., Weekes, C., & Gimenez, I.: Contrasting marine carbonate systems in two fjords in British
Columbia, Canada: Seawater buffering capacity and the response to anthropogenic CO2 invasion. PLoS One, 15(9), e0238432.
https://doi.org/10.1371/journal.pone.0238432, 2020.

Harrison, P. J., J. D. Fulton, F. J. R. Taylor, and T. R. Parsons.: Review of the biological oceanography of the Strait of Georgia:
1215   Pelagic environment. Can. J. Fish. Aquat. Sci., 40(7), 1064–1094. https://doi.org/10.1139/f83-129, 1983.

van Heuven, S., Pierrot, D., Rae, J.W.B., Lewis, E. R., and Wallace, D.W.R.: MATLAB Program Developed for CO2 System
Calculations. ORNL/CDIAC-105b. Carbon Dioxide Information Analysis Center, Oak Ridge National Laboratory, U.S.
Department of Energy, Oak Ridge, Tennessee. https://doi.org/10.3334/CDIAC/otg.CO2SYS_MATLAB_v1.1, 2011.
1220

Holden, J. J., Collicutt, B., Covernton, G., Cox, K. D., Lancaster, D., Dudas, S. E., et al.: Synergies on the coast: Challenges facing shellfish aquaculture development on the central and north coast of British Columbia. Marine Policy, 101, 108–117. https://doi.org/10.1016/j.marpol.2019.01.001, 2019.

1225   Hu, X., & Cai, W. J.: Estuarine acidification and minimum buffer zone: A conceptual study. Geophysical Research Letters, 40(19), 5176–5181. https://doi.org/10.1002/grl.51000, 2013.

Ianson, D., Allen, S. E., Harris, S. L., Orians, K. J., Varela, D. E., & Wong, C. S.: The inorganic carbon system in the coastal upwelling region west of Vancouver Island, Canada. Deep-Sea Research Part I: Oceanographic Research Papers, 50(8), 1023–

1230   1042. https://doi.org/10.1016/S0967-0637(03)00114-6, 2003.

Ianson, D., Allen, S. E., Moore-Maley, B. L., Johannessen, S. C., & Macdonald, R. W.: Vulnerability of a semi-enclosed estuarine sea to ocean acidification in contrast with hypoxia. Geophysical Research Letters, 43(11), 5793–5801. https://doi.org/10.1002/2016GL068996, 2016.

1235

Jarníková, T., Olson, E. M., Allen, S. E., Ianson, D., & Suchy, K. D.: A clustering approach to determine biophysical provinces and physical drivers of productivity dynamics in a complex coastal sea. Ocean Science Discussions, 1–36. https://doi.org/10.5194/os-2021-66, 2021.

1240   Jarníková, T., Ianson, D., Allen, S. E., Shao, A. E., & Olson, E. M.: Anthropogenic carbon increase has caused critical shifts in aragonite saturation across a sensitive coastal system. Global Biogeochemical Cycles, 36, e2021GB007024. https://doi.org/10.1029/2021GB007024, 2022.

Jiang L. Q, Carter B. R., Feely R. A., Lauvset S. K., Olsen A.: Surface ocean pH and buffer capacity: past, present and future.
1245   Sci Rep. 2019 Dec 9;9(1):18624. doi: 10.1038/s41598-019-55039-4, PMID: 31819102; PMCID: PMC6901524, 2019.

Kelly, R. P., Foley, M. M., Fisher W. S., Feely, R. A., Halpern, B. S., Waldbusser, G. G., Caldwell, M. R.: Mitigating Local Causes of Ocean Acidification with Existing Laws. Science, 332, 1036 – 1037, https://doi.org/10.1126/science.1203815, 2011.

1250   King, W. L., Jenkins, C., Seymour, J. R., & Labbate, M.: Oyster disease in a changing environment: Decrypting the link between pathogen, microbiome and environment. Marine Environmental Research, 143, 124 - 140. https://doi.org/10.1016/j.marenvres.2018.11.007, 2019.

Kroeker, K. J., Kordas, R. L., Crim, R. N., & Singh, G. G.: Meta-analysis reveals negative yet variable effects of ocean
1255 acidification on marine organisms. Ecology Letters, 13(11), 1419–1434. https://doi.org/10.1111/j.1461-0248.2010.01518.x,
2010.

LeBlond, P. H.: The Strait of Georgia: Functional anatomy of a coastal sea, Can. J. Fish. Aquat. Sci., 40(7), 1033–1063,
https://doi.org/10.1139/f83-128, 1983.
1260
Lewis, E. R., and Wallace D. W. R.: Program developed for CO2 system calculations, Rep. oRNL/CDIAC-105, U.S. Dep. Of
Energy, Oak Ridge, Tenn., 1998.

Lovenduski, N. S., Gruber, N., Doney, S. C., & Lima, I. D.: Enhanced CO2 outgassing in the Southern Ocean from a positive
1265 phase of the Southern Annular Mode. Global Biogeochemical Cycles, 21(2), https://doi.org/10.1029/2006GB002900, 2007.

Lowe, A. T., Bos, J., & Ruesink, J.: Ecosystem metabolism drives pH variability and modulates long-term ocean acidification
in the Northeast Pacific coastal ocean. Scientific Reports, 9(1), 963. https://doi.org/10.1038/s41598-018-37764-4, 2019.

1270 Masson, D.: Deep water renewal in the Strait of Georgia. Estuarine Coastal Shelf Sci., 54(1), 115–126,
doi:10.1006/ecss.2001.0833, 2002.

Millero, F., Graham, T. B., Huang, F., Bustos-Serrano, H. & Pierrot, D. : Dissociation constants of carbonic acid in seawater
as a function of salinity and temperature, Marine Chemistry, 100, 80-94, https://doi.org/10.1016/j.marchem.2005.12.001, 2006
1275
Millero, F.: Carbonate constants for estuarine waters. Mar Freshwater Res, 61, 139–142, https://doi.org/10.1071/MF09254,
2010.

Moore-Maley, B. L., Allen, S. E., & Ianson, D.: Locally driven interannual variability of near-surface pH and Ωa in the Strait
1280 of Georgia. Journal of Geophysical Research: Oceans, 121(3), 1600–1625, https://doi.org/10.1002/2015JC011118, 2016.

Moore-Maley, B. L., Ianson, D., & Allen, S. E.: Wind-Driven Upwelling and Seawater Chemistry in British Columbia's
Shellfish Aquaculture Capital. Canadian Meteorological and Oceanographic Society, https://bulletin.cmos.ca/upwelling-
seawater-chemistry-bc-shellfish-aquaculture, 2017.
1285
Moore-Maley, B. L., Ianson, D., & Allen, S. E.: The sensitivity of estuarine aragonite saturation state and pH to the carbonate
chemistry of a freshet-dominated river. Biogeosciences, 15(12), 3743–3760, https://doi.org/10.5194/bg-15-3743-2018, 2018.

Morin, E.: First-hand knowledge of BC ocean change: Oyster farmers' experiences of environmental change and oyster die-
1290   off events. Master's thesis, Simon Fraser University, Vancouver, Canada, Retrieved from http://rem-
main.rem.sfu.ca/theses/MorinEvie 2020 MRM751.pdf, 2020.

Morrison, J., Foreman, M. G. G., & Masson. D.: A method for estimating monthly freshwater discharge affecting British
Columbia coastal waters. Atmosphere - Ocean, 50(1), 1–8. https://doi.org/10.1080/07055900.2011.637667, 2011.
1295

Mucci, A.: The solubility of calcite and aragonite in seawater at various salinities, temperatures, and one atmosphere total
pressure. American Journal of Science, 283(7), 780–799. https://doi.org/10.2475/ajs.283.7.780, 1983.

NASA.: The Strait of Georgia turns milky green due to an "unprecedented" explosion of coccolithophores. Earth Observatory.
1300   https://earthobservatory.nasa.gov/images/88687/canadian-waters-teem-with-phytoplankton, 2016.

Natural   Resources   Canada.:   Canada   west   coast   topo-bathymetric   digital   elevation   model,
https://open.canada.ca/data/en/dataset/e6e11b99-f0cc-44f7-f5eb-3b995fb1637e, 2021.

1305   NOAA.: National Oceanic and Atmospheric Administration, National Geophysical Data Center. ETOPO1 1 Arc-Minute
Global   Relief   Model.   NOAA   National   Centers   for   Environmental   Information.
https://www.ncei.noaa.gov/access/metadata/landing-page/bin/iso?id=gov.noaa.ngdc.mgg.dem:316, 2009.

NOAA.: National Oceanic and Atmospheric Administration. Shorelines. Global Self-consistent Hierarchical High-resolution
1310   Geography Database. https://www.ngdc.noaa.gov/mgg/shorelines, 2017.

Olson, E. M., Allen, S. E., Do, V., Dunphy, M., & Ianson, D.: Assessment of nutrient supply by a tidal jet in the northern Strait
of Georgia based on a biogeochemical model. Journal of Geophysical Research: Oceans, 125(8), 1–25.
https://doi.org/10.1029/2019JC015766, 2020.
1315

Orr, J. C., Fabry, V. J., Aumont, O., Bopp, L., Doney, S. C., Feely, R. A., et al.: Anthropogenic ocean acidification over the
twenty-first century and its impact on calcifying organisms. Nature, 437(7059), 681–686. https://doi.org/10.1038/nature04095.
2005.

1320   Orr, J. C., Epitalon, J.-M., Dickson, A. G., & Gattuso, J.-P.: Routine uncertainty propagation for the marine carbon dioxide
system, Mar. Chem., 207, 84-107, doi:10.1016/j.marchem.2018.10.006, 2018.

Pacella, S. R., Brown, C. A., Waldbusser, G. G., Labiosa, R. G., & Hales.: Seagrass habitat metabolism increases short-term extremes and long-term offset of CO2 under future ocean acidification. Proceedings of the National Academy of Sciences of
1325 the United States of America, 115(15), 3870–3875. https://doi.org/10.1073/pnas.1703445115, 2018.

Pawlowicz, R., O. Riche, and M. Halverson.: The circulation and residence time of the Strait of Georgia using a simple mixing-box approach, Atmos. Ocean, 45(4), 173–193, doi:10.3137/ao.450401, 2007.

1330 Pawlowicz, R., Suzuki, T., Chappell, R., Ta, A., and Esenkulova, S.: Atlas of oceanographic conditions in the Strait of Georgia (2015– 2019) based on the Pacific Salmon Foundation's Citizen Science Dataset, Canadian Technical Report of Fisheries and Aquatic Sciences, 3374, ISBN 9780660349367, 2020.

Peña, M. A., Nemcek, N., & Robert, M.: Phytoplankton responses to the 2014–2016 warming anomaly in the northeast
1335 subarctic Pacific Ocean. Limnology and Oceanography, 64(2), 515-525. https://doi.org/10.1002/lno.11056, 2018.

Raven, J., Caldeira, K., Elderfield, H., Hoegh-Guldberg, O., Liss, P., et al. : Ocean acidification due to increasing atmospheric carbon dioxide. Royal Society, London, ISBN 0 85403 617 2, 2005. https://royalsociety.org/-/media/Royal_Society_Content/policy/publications/2005/9634.pdf.

1340
Rivero-Calle, S., Gnanadesikan, A., Del Castillo, C. E., Balch, W. M., & Guikema, S. D. Multidecadal increase in North Atlantic coccolithophores and the potential role of rising CO2. Science, 350, 1533–1537. https://doi.org/10.1126/science.aaa8026, 2015.

1345 Sabine, C. L., Feely, R. A., Gruber, N., Key, R. M., Lee, K., Bullister, J. L., & Rios, A. F. The oceanic sink for anthropogenic CO2. Science, 305(5682), 367–371. https://doi.org/10.1126/science.1097403, 2004.

Salisbury, J., Green, M., Hunt, C., Campbell, J., Growth, S., & Rivers, A.: Coastal acidification by rivers: A threat to shellfish? Eos, 89(50), 513, 2008.
1350
Sarmiento, J. L., & Gruber, N.; Ocean biogeochemical dynamics. Princeton University Press, 2006.

Silver, J. J.: Shellfish and coastal change: Pacific oysters and manila clams in BC waters. BC Studies: The British Columbian Quarterly, (181), 83–103, 2014.
1355

Simpson, E., Ianson, D., & Kohfeld, K. E.: Using end-member models to estimate seasonal carbonate chemistry and acidification sensitivity in temperate estuaries. Geophysical Research Letters, 49(2), e2021GL095579. https://doi.org/10.1029/2021gl095579, 2022.

1360   Spalding, C., Finnegan, S., & Fischer, W. W.: Energetic costs of calcification under ocean acidification. Global Biogeochemical Cycles, 31(5), 866–877. https://doi.org/10.1002/2016GB005597, 2017.

Stenzel, H. B.: Oysters: Composition of the larval shell. Science, 145, 155–156, 1964.

1365   Thomson, R. E.: Oceanography of the British Columbia Coast. Canadian Special Publication of Fisheries and Aquatic Sciences, 56. Retrieved from http://www.ncbi.nlm.nih.gov/pubmed/2837640, 1981.

Turi, G., Lachkar, Z., Gruber, N., & Munnich, M.: Climatic modulation of recent trends in ocean acidification in the California Current System. Environmental Research Letters, 11(1), 014007. https://doi.org/10.1088/1748-9326/11/1/014007, 2016.

1370

Uppström, L. R.: The boron/chlorinity ratio of deep-sea water from the Pacific Ocean. Deep-Sea Research and Oceanographic Abstracts, 21(2), 161–162. https://doi.org/10.1016/0011-7471(74)90074-6, 1974.

Waldbusser, G. G., & Salisbury, J. E.: Ocean acidification in the coastal zone from an organism's perspective: Multiple system
1375   parameters, frequency domains, and habitats. Annual Review of Marine Science, 6(1), 221-247. https://doi.org/10.1146/annurev-marine-121211-172238, 2014.

Waldbusser, G. G., Hales, B., Langdon, C. J., Haley, B. A., Schrader, P., Brunner, E. L., et al.: Saturation-state sensitivity of marine bivalve larvae to ocean acidification. Nature Climate Change, 5(3), 273-280. https://doi.org/10.1038/nclimate2479,
1380   2015.

Waldbusser, G. G., Gray, M. W., Hales, B., Langdon, C. J., Haley, B. A., Gimenez, I., Smith, S. R., Brunner, E. L., & Hutchinson, G.: Slow shell building, a possible trait for resistance to the effects of acute ocean acidification. Limnology and Oceanography, 61, 1969-1983. https://doi.org/10.1002/lno.10348, 2016.

1385

Waldichuk, M.: Physical oceanography of the Strait of Georgia, British Columbia. Fisheries Research Board of Canada Bulletin, 14, 321-486. https://doi.org/10.1139/f57-013, 1957.

Waldichuk, M.: Dispersion of Kraft-Mill Effluent from a Submarine Diffuser in Stuart Channel, British Columbia. Journal of
1390   the Fisheries Research Board of Canada, 21(5), 1289-1316. https://doi.org/10.1139/f64-107, 1964.

Wallace, R. B., Baumann, H., Grear, J. S., Aller, R. C., & Gobler, C. J.: Coastal ocean acidification: The other eutrophication
problem. Estuaries and Coasts, 37, 1-13. https://doi.org/10.1007/s12237-013-9693-0, 2014.

1395   Wendling, C. C., Batista, F. M., & Wegner, K. M.: Persistence, seasonal dynamics and pathogenic potential of Vibrio
communities from Pacific oyster hemolymph. PLoS One, 9(2), e94256. https://doi.org/10.1371/journal.pone.0094256, 2014.

White, R.H., Anderson, S., Booth, J.F. et al. The unprecedented Pacific Northwest heatwave of June 2021. Nat Commun **14**,
727. https://doi.org/10.1038/s41467-023-36289-3, 2021.

1400

WOCE. Hydrographic Programme Operations and Methods. WOCE Report, 15, 1991.